THE ROLE OF VITAMIN E HYDROXYLASES IN VITAMIN E METABOLISM AND STATUS

A Dissertation

Presented to the Faculty of the Graduate School

of Cornell University

in Partial Fulfillment of the Requirements for the Degree of

Doctor of Philosophy

by

Sabrina Anne Bardowell

August 2012

THE ROLE OF VITAMIN E HYDROXYLASES IN VITAMIN E METABOLISM AND STATUS

Sabrina Anne Bardowell, Ph.D.

Cornell University 2012

Vitamin E is a group of compounds that are considered to be the most important lipophilic antioxidants, however there is still much unknown about the biological actions of the various forms of vitamin E as well as the mechanisms that influence the concentration of vitamin E forms in tissues. Despite the common predominance of mainly γ-tocopherol (γ-TOH) in the diet, α-TOH is present in serum and tissues at levels 5-6 times that of γ-TOH. The biological rational for this selectivity remains an enigma. The focus of this work was on the selective post-absorptive catabolism of non-α-TOH forms via the vitamin E-ω-oxidation pathway. Cytochrome P450 4F2 (CYP4F2) is the only known human enzyme shown to display TOH-ω-hydroxylase activity. In an effort to investigate the role of TOH-ω-hydroxylase activity in vitamin E metabolism and status, the functional murine ortholog of *CYP4F2* was identified and the consequences of its deletion on vitamin E metabolism and status were determined. *In vivo* and *in vitro* studies revealed Cyp4f14 to be the major, but not the only, vitamin E-ω-hydroxylase in mice, and to have critical function in regulating body-wide vitamin E status. Disruption of *Cyp4f14* expression resulted in hyper-accumulation of γ-TOH in mice fed a soybean oil diet in which the major tocopherol was γ-TOH. Supplementation of *Cyp4f14*$^{-/-}$ mice with high levels of δ- and γ-TOH exacerbated the tissue enrichment of these forms of vitamin E. Through the use of

metabolic cage studies, previously unappreciated mechanisms of vitamin E elimination were discovered, which served to counterbalance the metabolic deficit observed in *Cyp4f14*$^{-/-}$ mice. Fecal elimination of unmetabolized TOHs was determined to be a high capacity mechanism to be minimize diet induced accumulation of TOHs, especially at high dietary levels. Additionally, novel ω-1 and ω-2 vitamin E hydroxylase activities were discovered and were found to quantitatively important vitamin E elimination mechanisms. *Cyp4f14*$^{-/-}$ mice also revealed the existence of other hepatic TOH-ω-hydroxylase enzyme(s). Therefore genetically modified mice, in which no CYP activity was present in the liver, were utilized in order to eliminate all hepatic vitamin E metabolism. Metabolic cage studies revealed the presence of vitamin E hydroxylase activity in non-hepatic tissues. Mouse and human small intestine mucosa were found to have TOH-ω-hydoxylase activity, representing at least one site of extra-hepatic vitamin E metabolism. Lastly, the use of cell culture studies demonstrated that two polymorphisms in CYP4F2 functionally alter TOH-ω-hydroxylase activity, which may play a role in vitamin E status in humans. Overall, the current works lends new insights into the physiological role of the TOH-ω-oxidation pathway as well as reveals novel mechanisms of vitamin E metabolism in both mice and humans, which play an important role in the regulation of vitamin E status.

BIOGRAPHICAL SKETCH

Sabrina Anne Bardowell was born in Fort Lauderdale, Florida in 1984, and lived there until moving to Miami, Florida for her undergraduate work at Florida International University. Sabrina received her B.S. in Dietetics and Nutrition with a minor in Chemistry, and graduated Summa Cum Laude in 2007. During her undergraduate career, Sabrina was an NIH-MBRS/RISE Scholar for two years, conducting research in an Organic Chemistry laboratory on the topic of the detection of blue-green algae toxins in dietary supplements. Additionally, she did a dietetic internship through FIU and gained registered dietitian (RD) status in 2007.

Immediately following her undergraduate degree, Sabrina moved to Ithaca, New York to pursue a Ph.D. in Nutritional Sciences at Cornell University, with minors in Epidemiology and Genomics. During her time at Cornell, Sabrina has been a teaching assistant as well as given guest lectures for many courses including Methods in Nutritional Sciences and Physiological and Biochemical Basis of Nutrition. For several years, Sabrina was funded through an NIH Training Grant, during which time she conducted research and presented her research at several departmental seminars and scientific conferences.

This work is dedicated to:

My family for their unconditional love, support, and belief in me.

Bob Parker, who started as a mentor and ended as family.

The friends that have experienced the past 5 years with me.

God, my father, for giving me immeasurably more than I could ask or imagine.

ACKNOWLEDGMENTS

The pages written here do not only describe the culmination of years of research, but also reflect many relationships, without which, this work would never have been completed.

First and foremost, my advisor Bob Parker, has spent countless hours teaching and training me, and working side by side with me. I have learned from him to be a thorough scientist, who doesn't take the path of least resistance just because it's easier, and who is open-minded enough to see outside of my own perspective.

The members of my committee, Pat Cassano, Kimberly O'Brien, and Zhenglong Gu, have provided their precious time and attention, thoughtful criticism, and encouraging words throughout the past five years.

Angelos Sikalidis and Heather Roman taught me many molecular techniques and Heather taught me how to maintain a large mouse colony. John LaBarre helped in the lab for several years and conducted some of the vitamin E analysis described in this dissertation. Francoise Vermeylen of the Cornell Statistical Consulting Unit has continually provided invaluable statistical assistance. Dr. Lynn Ulatowski kindly performed α-TTP Western blotting for these studies. We also thank Dr. Robin Davisson for the use of her mouse metabolic cages, which were indispensible to this work.

Many collaborators participated in this work and were co-authors on manuscripts from each chapter. Co-authors from Chapter 1: Faping Duan from the Department of Biological and Environmental Engineering at Cornell University, Danny Manor from the Departments of Nutrition and Pharmacology at Case Western Reserve University, and Joy Swanson from the Division of Nutritional Sciences at Cornell University. Co-author from Chapter 2: Xinxin Ding from the Wadsworth Center at the New York State Department of Health. Co-author from Chapter 3: David Stec from the Department of Physiology and Biophysics from the University of Mississippi Medical Center.

This work was financial supported by National Institutes of Health DK007158 and by the Division of Nutritional Sciences at Cornell University.

Lastly, some wonderful friends have provided listening ears, shoulders to cry on, and some much needed fun and distraction, all of which have been crucial to the completion of this work. The list is too long to mention here, but I would like to especially thank Carly Pacanowski who has been with me through this journey from the beginning to the end.

TABLE OF CONTENTS

LIST OF FIGURES

LIST OF TABLES

LIST OF ABBREVIATIONS

TOH	tocopherol
T3	tocotrienol
α-TTP	α-tocopherol transfer protein
VLDL	very low density lipoprotein
AVED	ataxia with vitamin E deficiency
CYP4F2	cytochrome P450 4F2
CYP	cytochrome P450
Cpr	cytrochrome P450 reductase
SNP	single nucleotide polymorphism
LTB4	leukotriene B4
PMSF	phenylmethanesulfonylfluoride
NaP	sodium phosphate
DTT	Dithiothreitol
BSA	bovine serum albumin
GC-MS	gas chromatography-mass spectrometry
MTBE	methyl tert-butyl ether
BSTFA	N,O-Bis(trimethylsilyl)trifluoroacetamide
TMS	tri-methyl silyl
HCl	hydrochloric acid
L-*Cpr*	liver-specific cytochrome P450 reductase disruption
AA	arachidonic acid
20-HETE	20-hydroxyeicosatetraenoic acid

LIST OF SYMBOLS

α	alpha
γ	gamma
δ	delta
ω	omega

INTRODUCTION

Vitamin E is a family of chemically-related lipophilic compounds, comprised of tocopherols (TOHs) and tocotrienols (T3s), which differ in the number and position of the methyl groups around the chromanol ring and in the saturation and stereochemistry of the phytyl tail (**Fig. I.1**). First discovered in 1922 to be required for fertility in rats (*1*), these compounds are considered to be the most important liphophilic radical-quenching antioxidants in cell membranes and lipid stores. While all forms of vitamin E possess roughly similar radical scavenging activity *in vitro* (*2, 3*), α-TOH has been the focus of research due to the fact that it is the form that is found in the highest concentration in plasma and tissues of animals.

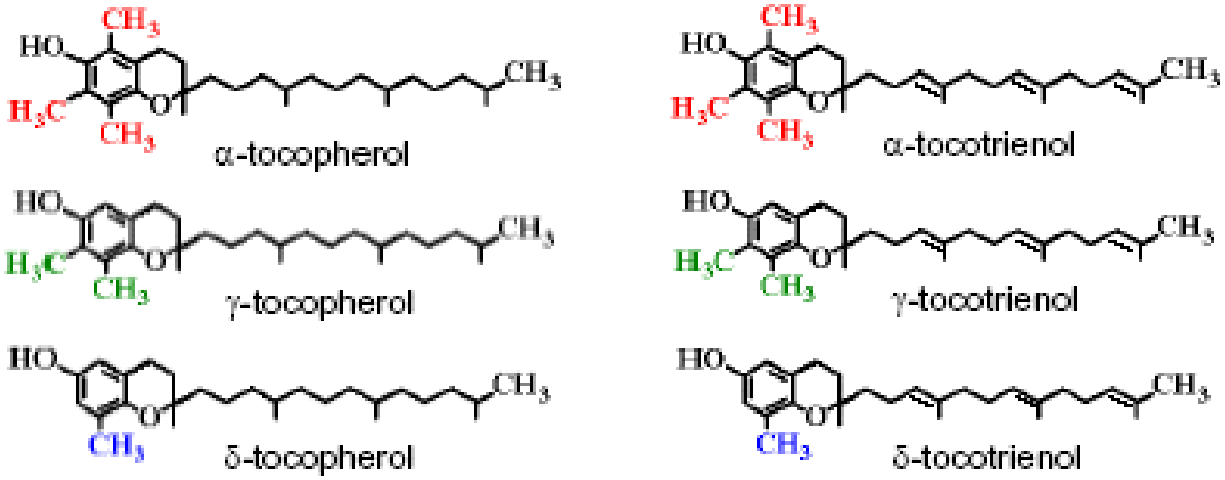

Fig. I.1. The chemical Structure of vitamin E. α-, γ-, and δ-TOH have 3, 2 and 1 methyl groups on the polar head of the compound, respectively. The corresponding T3s have three double bonds in the side chain of the compound.

Vitamin E is synthesized in plants and is consumed in humans largely through vegetable oils; the content and ratio of vitamin E forms varies by oil. The typical North American diet contains 2-4 times as much γ-TOH compared to α-TOH (*4, 5*) due to the prevalence of corn and

soybean oils. Despite the consumption of mainly γ-TOH, α-TOH is present in serum and tissues at levels 5-6 times that of γ-TOH (*6*). The preferential accumulation of α-TOH ("the α-TOH phenotype") is widespread in the animal kingdom and yet the biological advantage of this phenotype is currently unknown. The α-TOH phenotype is thought to be brought about by two mechanisms: the α-tocopherol transfer protein (α-TTP) and the vitamin E-ω-oxidation pathway, although the relative contribution of these mechanisms to the α-TOH phenotype has not been investigated.

All forms of vitamin E are absorbed apparently to the same extent and transported in the plasma via lipoproteins. Vitamin E is taken up by the liver with lipoproteins and is thought to be resecreted into the plasma via very low density lipoproteins (VLDL). α-TTP, a cytosolic liver protein, is thought to facilitate the resecretion of TOHs from the liver into the plasma for transport to peripheral tissues (*7, 8*). The relative affinities of α-TTP to the various forms of vitamin E is thought to play a major role in controlling vitamin E levels in the plasma and tissues. α-TTP has the highest affinity for RRR-α-TOH *in vitro*, and much lower affinity for other TOHs and T3s (*9*), thereby presumably contributing to the preferential retention of α-TOH in animal tissues (*10, 11*). While it is still unclear the extent to which α-TTP can bind to and facility the secretion of non-α-TOH forms in the body, studies in which α-TTP has been disrupted in mice certainly demonstrates the importance of α-TTP in maintaining plasma and tissue α-TOH levels. α-TTP knockout mice display severe vitamin E deficiency and neurological symptoms that can be overcome by large dietary doses of α-TOH (reviewed in (*12*)). Indeed, humans with genetic defects in α-TTP display severe vitamin E deficiency as well as neurological abnormalities, termed ataxia with vitamin E deficiency (AVED) (*13*).

The second mechanism that is involved in the α-TOH phenotype is the preferential post-absorptive catabolism of non-α-TOH forms of vitamin E via the vitamin E-ω-oxidation pathway (**Fig. I.2**). The first and rate limiting step of the vitamin E-ω-oxidation pathway of vitamin E metabolism is the ω-hydroxylation of one of the two terminal (13') methyl groups on the phytyl side chain of TOHs and T3s. ω-Hydroxylation is followed by oxidation to the carboxy form and a series of side chain shortening steps, ultimately leading to short-chain, water soluble metabolites that can be excreted in the urine (*14*). Although the most commonly studied metabolites are the shortest-chain metabolites (3'- and 5'-COOH), this pathway can produce seven metabolites, including the original 13'-OH product, the 13'-COOH product, and five subsequent n-2 COOH products.

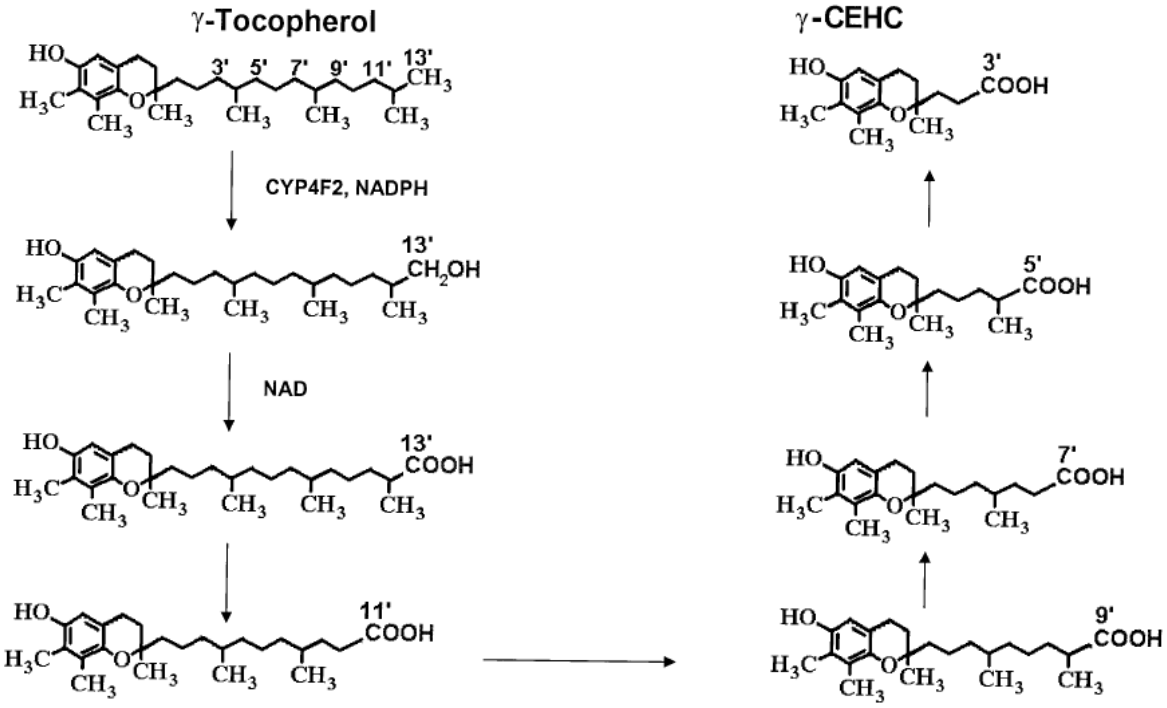

Figure I.2 The TOH-ω-oxidation pathway of γ-TOH. The first and rate-limiting step of the TOH-ω-oxidation pathway of vitamin E metabolism is the ω-hydroxylation of one of the terminal methyl groups of the compound, followed by oxidation to the carboxy form, and a series of side-chain shortening steps, leading to water-soluble metabolites that can be excreted in the urine.

The human cytochrome P450 4F2 (CYP4F2) expressed predominantly in liver has been identified as a human vitamin E-ω-hydroxylase (*14*). The cytochrome P450 (CYP) superfamily of enzymes catalyze a vast number of catalytic reactions, including the metabolism of lipids, steroids, and xenobiotics. These endoplasmic reticulum-bound enzymes require NADPH and the co-enzyme cytochrome P450 reductase (CPR) for the source and transfer of electrons to the CYP enzyme. While enzymatic redundancy is common within in the P450 family, CYP4F2 is the only known enzyme to have vitamin E-ω-hydroxylase activity (*14*). Importantly, CYP4F2 displays substrate preference, such that non-α-TOH forms of vitamin E are metabolized to a greater extent than α-TOH, thereby potentially contributing to the α-TOH phenotype. Specifically, T3s are metabolized to the greatest extent by CYP4F2, followed by δ-TOH, γ-TOH, and lastly α-TOH which is metabolized less efficiently than all other forms of vitamin E (*15*).

This dissertation was aimed at determining the role of TOH-ω-hydroxylase activity in vitamin E metabolism and status through the use of two knockout mouse models: 1) disruption of *Cyp4f14*, a mouse ortholog of *CYP4F2* and 2) a liver-specific disruption of the *Cpr gene*, (*L-Cpr*) eliminating all CYP activity in the liver. Additionally, we characterized the functional effect of two common non-synonymous single nucleotide polymorphisms (SNPs) in the human CYP4F2 gene on TOH-ω-hydroxylase activity. Collectively, this work clarifies the importance of the TOH-ω-oxidation pathway as well as illuminates novel pathways and mechanisms in preventing accumulation of non-α-TOH forms of vitamin E.

CHAPTER 1

DISRUPTION OF MOUSE CYTOCHROME P450 4f14 (*Cyp4f14*) CAUSES SEVERE PERTURBATIONS IN VITAMIN E METABOLISM

Introduction

Vitamin E is a family of hydrophobic 6-hydroxy chromanols synthesized by plants whose function is thought to be the scavenging of lipophilic free radicals in cell membranes or lipid stores. Of nine known family members, several, particularly the tocopherols with saturated side chains, are common in the diet. However, while all possess roughly similar radical scavenging activity in vitro (*2, 3*), one, α-tocopherol (α-TOH), preferentially accumulates in animal tissue. While the typical North American diet contains 2-4 times as much γ-TOH as compared to α-TOH due to the prevalence of soybean and corn oils (*4, 5*), α-TOH is present in serum at levels 5-6 times that of γ-TOH (*6*). This preferential accumulation of α-TOH (the "α-TOH phenotype") is widespread throughout the animal kingdom; however the biological advantage of this conservation remains an enigma. The preferential accumulation of α-TOH is apparently facilitated by two activities: preferential retention of α-TOH by the hepatic tocopherol transfer protein (α-TTP) (*9, 16*), and extensive post-absorptive catabolism of vitamers other than α-TOH by vitamin E-ω-hydroxylase (*15*). The relative contribution of these two activities *in vivo* has not been investigated. Vitamin E-ω-hydroxylase activity has been observed in Drosophila, with similar substrate specificity to that of the human activity, suggestive of a biological importance and evolutionary advantage of this highly conserved activity (*17*).

We previously identified cytochrome P450 4F2 (CYP4F2) as a human vitamin E-ω-hydroxylase (*18*). CYP4F2 catalyzes the ω-hydroxylation of one of the terminal methyl groups of the 16-carbon branched side chain of tocopherols and tocotrienols (T3s, with three double

bonds in the side chain). This oxidation is the first and rate-limiting step in the ω-oxidation pathway of vitamin E catabolism, and represents the only reported enzyme-mediated pathway of vitamin E metabolism. Following the initial ω-hydroxylation event, tocopherols and tocotrienols undergo a series of side chain shortening steps, analogous to fatty acid β-oxidation, yielding short chain carboxychromanol metabolites that are excreted in urine (*19-21*). In the human, CYP4F2 is expressed predominantly in the liver (*22*), and was initially identified as a ω-hydroxylase of leukotriene B4 (LTB4). While several human CYP enzymes other than CYP4F2 have been shown to ω-hydroxylate LTB4, including CYP4F3A (leukocyte) and CYP4F3B (liver)(*23*), CYP4F2 remains the only human enzyme demonstrated to metabolize vitamin E.

We hypothesized that TOH-ω-hydroxylase activity is essential for establishing and maintaining the α-TOH phenotype. To test this hypothesis, we sought to identify the ortholog of *CYP4F2* in mice, disrupt its expression by homologous recombination, and determine the consequences of its ablation on tocopherol metabolism and status.

Experimental Procedures

Materials - Trizol reagent, Superscript First Strand Synthesis Kit, pcDNA3.1/Hygro+ and Platinum PCR Supermix High Fidelity were purchased from Invitrogen (Carlsbad, CA), and primers from Integrated DNA Technologies (Coralville, Iowa). QIA Shredder Spin Columns, RNeasy Mini Kit, and RNase-free DNase were purchased from Qiagen (Valencia, CA). High Capacity cDNA Reverse Transcription Kit, Taqman Universal Master Mix and all Taqman assays were obtained from Applied Biosystems (Foster City, CA). Rabbit anti-human CYP4F2 antibody and pre-immune (control) IgG were purchased from Research Diagnostics (Concord, MA). Tocopherols were obtained from Matreya, LLC (Pleasant Gap, PA). γ-T3 was a gift from Volker Berl (BASF Global, Schwarzheide, Germany). The internal standards d_9-α-TOH and d_9-

α-CEHC were custom synthesized by J. Swanson (Cornell University, Ithaca, NY). Pyridine and N, O-Bis-[trimethylsilyl]trifluoracetamide containing 1% trimethylchlorosilane were purchased from Pierce Chemical (Rockford, IL). COS-7 cells were obtained from American Type Culture Collection (Manassas, VA). Sesamin was acquired from Cayman Chemical (Ann Arbor, MI), and bovine serum albumin, NADPH, β-glucuronidase (from *Escherichia coli*), and sulfatase (from *Aerobacter aerogenes*) were purchased from Sigma-Aldrich (St. Louis, MO). Wild type C57B/6J mice were obtained from Jackson Laboratory (Bar Harbor, ME). Rodent chow (Teklad 7912) was purchased from Teklad Diets (Madison, WI) and modified AIN-93G rodent diet was manufactured by DYETS Inc (Bethlehem, PA).

Immunoinhibition of mouse liver microsomal TOH-ω-hydroxylase by anti-human CYP4F antibody - Microsomes were prepared from fresh mouse liver by standard differential centrifugation. Liver was minced and homogenized using a Teflon/glass homogenizer in five volumes ice cold 15 mM HEPES buffer containing 0.25 M sucrose, 1 mM EDTA, and 1 mM phenylmethanesulfonylfluoride [PMSF], pH 7.4), then centrifuged at 10,000 x g for 20 min at 4˚C. The supernatant was centrifuged at 100,000 x g for 1 h at 4˚C. The microsomal pellet was resuspended in 0.1 mM sodium phosphate (NaP) buffer containing 1 mM EDTA, 0.1 mM Dithiothreitol (DTT) and 20% glycerol. Microsomal protein concentration was determined by a Bradford-based Bio-Rad assay using bovine serum albumin (BSA) as the standard. Microsomes were pre-incubated with 1, 8, or 25 μg of anti-human CYP4F2 IgG antibody or 25 μg pre-immune (control) IgG for 30 min on ice. TOH-ω-hydroxylase activity was determined as previously described (*18*), using 60 μM δ-TOH-BSA complex as substrate.

BLAST comparison of human CYP4F2 with muring Cyp sequences - A comparison of the protein sequence of human CYP4F2 (NCB Accession #AAC27730.1) with that of all

reported murine proteins was conducted using the BLASTP program (http://blast.ncbi.nlm.nih.gov/Blast.cgi) and the RefSeq protein database. A BLAST comparison of the amino acid sequence of the putative substrate binding domain of CYP4F2 (residues 69-115, (*24*)), was also conducted. Two Cyp enzymes reported to be expressed in murine liver, Cyp4f14 and Cyp4f15 (*25*), were selected for further investigation based on high levels of homology with human CYP4F2.

Cloning, expression, and assessment of TOH-ω-hydroxylase activity of Cyp4f14 and Cyp4f15 - Total RNA was extracted from mouse liver using Trizol reagent and reverse transcribed using Superscript First Strand Synthesis Kit. *Cyp4f14* and *Cyp4f15* cDNA was amplified from mouse liver RNA by one-step RT-PCR using primers based on the published sequences of murine liver *Cyp4f14* cDNA (*26*) (GenBank Accession Number AB037541) and *Cyp4f15* (GenBank Accession Number BC021377). The cDNA was restricted and ligated into pCDNA3.1/Hygro+ vector using the HndIII and Xho I restriction enzymes, and correct sequences confirmed by sequencing. The *Cyp4f14* and *Cyp4f15* genes (in the pCDNA3.1/Hygro+) were transfected into COS-7 cells. Forty-eight hours post-transfection, cells were exposed to hygromycin (200 μg/ml). Discrete colonies were picked after about 3 weeks in the selection media. Expression of Cyp4f14 and Cyp4f15 protein was verified by Western blotting using anti-CYP4F2 antibody which cross-reacts with other CYP4F (human) and Cyp4f (mouse) enzymes due to the high sequence homology, according to the manufacturer.

Total cell membrane fractions from homogenates of COS-7 cultures were prepared by ultracentrifugation (100,000 x g). TOH-ω-hydroxylase activity was assessed in aliquots of COS-7 cell membranes using δ-TOH as substrate as previously described (*18*). Preparations were compared at similar Cyp4f14/4f15 protein expression levels as determined by Western blot.

TOH-ω-hydroxylase activity and sesamin sensitivity of murine Cyp4f14 in COS-7 cells - A COS-7 clone expressing Cyp4f14 was incubated with a mixture of 20 μM each α-TOH, γ-TOH, and δ-TOH, with or without 1 μM sesamin, for 48 h. Media was extracted and assayed for the presence of ω-oxidation metabolites of the three substrate tocopherols by gas chromatography-mass spectrometry (GC-MS) as previously described (*27*).

Generation of Cyp4f14-null mice - The gene targeting vector was designed to target exons 2-5, which includes the putative substrate binding domain of Cyp4f14 (*24*), with the insertion of an IRES/LacZ/Neo/PolyA cassette to allow the tracing of gene expression (**Fig. 1.1**). Murine 129/SvEv embryonic stem cells were transfected, and integration of the genomic construct at the predicted site within the *Cyp4f14* locus was confirmed by long-distance PCR using probes external to the targeted region (3' homologous arm and 5' homologous arm). Following ES cell expansion and karyotyping, selected clones were microinjected into C57BL/6 blastocysts and implanted into psuedopregnant female mice. Male germline chimeras carrying a *Cyp4f14* mutant allele were backcrossed with wild-type C57BL/6J females. Heterozygous F1 progeny were intercrossed to obtain F2 mice that were homozygous wild-type ($Cyp4f14^{+/+}$), heterozygous null ($Cyp4f141^{+/-}$) and homozygous null ($Cyp4f14^{-/-}$) for the targeted allele. Use of mice was in accordance with protocols approved by the Cornell Institutional Animal Care and Use Committee and following the National Institutes of Health guidelines for laboratory animal use.

Genotyping of Cyp4f14 deficient mice - Genomic DNA was prepared from 0.2 cm tail snips using the HotSHOT method (*28*). Genomic DNA (50-200 ng) was used directly for PCR

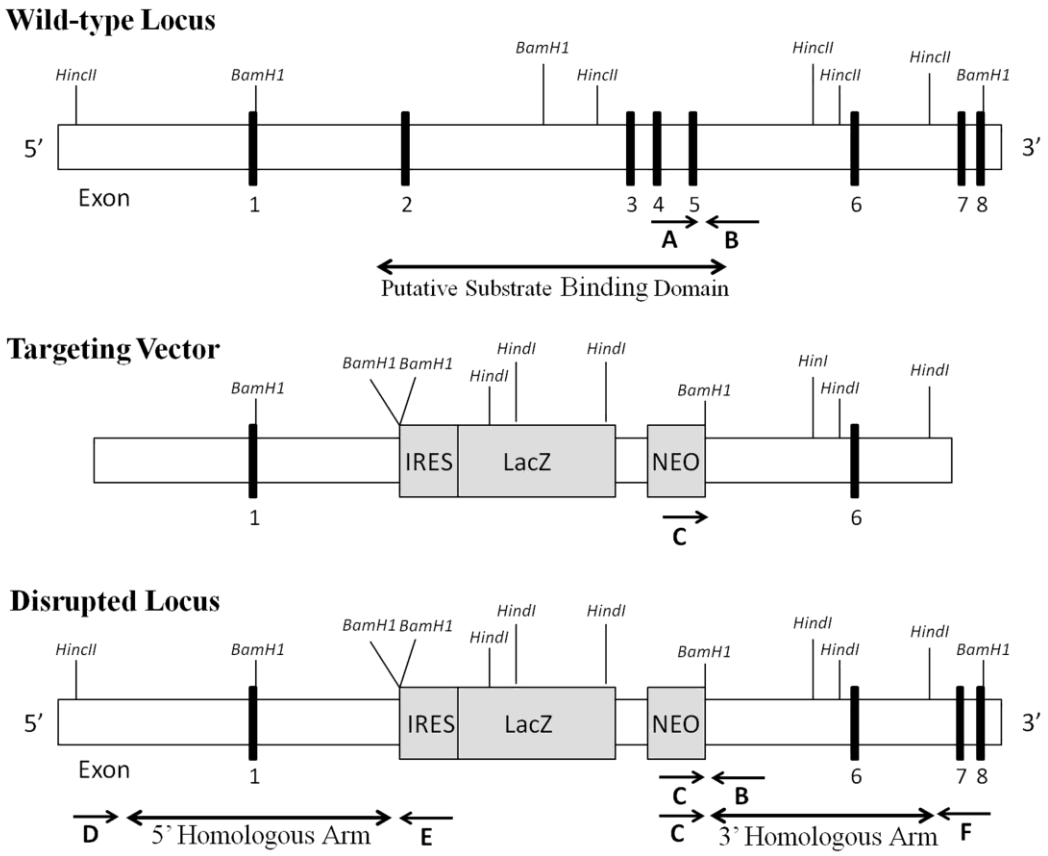

Figure 1.1. Strategy of disruption of *Cyp4f14* in the mouse. Genomic structure of *Cyp4f14* locus (top), the *Cyp4f14* gene targeting construct containing a IRES/ LacZ/Neo/PolyA cassette (middle), and the disrupted locus in which exons 2-5 have been replaced (bottom). The arrows marked A, B, and C show the location of primers used for confirmation of germline transmission and tail snip genotyping. The arrows marked C, D, E, and F indicate the location of primers used for long distance PCR analysis, confirming the integration of the targeting construct into the *Cyp4f14* locus.

amplification with Platinum PCR SuperMix High Fidelity. Wild-type primers CTGGACATGTTTGAGCACG (forward; primer A) and GAACCACAGGCTAAGTCCATC (reverse; primer B) and a primer specific for the neomycin insert TCTGGATTCATCGACTGTGG (forward; primer C) were used for PCR amplification. The cycling protocol was as follows: 94˚C, 2 min (1 cycle); 94˚C, 15 s; 60˚C, 30 s; 68˚C, 1 min (35

cycles) and 68˚C, 7 min (1 cycle). The PCR products were separated on a 2% agarose gel yielding a 365 bp band for wild-type mice and 480 bp band for *Cyp4f14*-null mice (**Fig. 1.3A**).

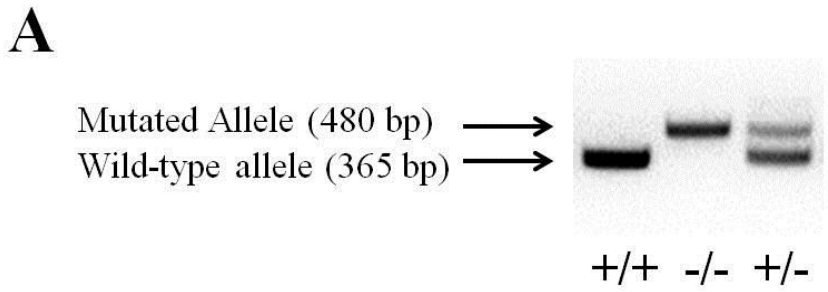

Figure 1.3A. PCR genotyping of *Cypf14* animals. Tail DNA was extracted from F2 littermates of a heterozygous cross and subjected to PCR using primers specific for the wild-type (365 bp) and mutated (480 bp) alleles.

Experimental diets - Initial studies were conducted in mice fed Teklad 7912, a commercial chow-type diet containing low concentrations of δ- and γ-TOH. Subsequent studies utilized a modified AIN-93G semipurified diet designed to be rich in γ-TOH in the form of soybean oil, the most prevalent vegetable oil in North America. Samples of diets were ground using a mortar and pestle and lipids were extracted using hexane-methyl tert-butyl ether (MTBE) (2:1). Lipid extracts were dried and derivatized using pyridine and N,O-Bis(trimethylsilyl)trifluoroacetamide (BSTFA)/1% tri-methy silyl (TMS), and tocopherols quantified by GC-MS using d_9-α-TOH as internal standard. Tocopherol content of the chow and soybean oil diets, hereafter referred to as γT-10 and γT-165 denoting their respective concentration of γ-TOH is presented in **Table 1.1**.

Feeding studies - Mice of all three genotypes weaned onto the γT-10 diet at 21 days of age were fed the diet for three weeks. *Cyp4f14*$^{+/+}$ and *Cyp4f14*$^{-/-}$ mice weaned onto the γT-165 diet were fed the diet for six weeks. At the end of the feeding periods, mice were deeply

Table 1.1
Dietary Tocopherol Composition

Lipids were extracted from each diet and vitamin E was quantified by GC-MS using d_9-α-TOH as internal standard.

Diet	Vitamin E (mg/kg)			
	δ-TOH	γ-TOH	α-TOH	α-T acetate
γT-10 Diet	9	10	10	150
γT-165 Diet	83	165	12	0

anesthetized by isoflurane inhalation and exsanguinated via cardiac puncture. Heparinized blood was centrifuged at 6,000 x g for 5 min, and serum frozen at -80˚C until analysis. Liver tissue samples were flash frozen in liquid nitrogen for RT-PCR and vitamin E analysis. The remainder of the liver was immediately used for microsomal preparation as described above. Samples of additional tissues (kidney, lung, heart, testis, muscle [psoas major], abdominal fat) were flash frozen for vitamin E analysis.

24-Hour urine and fecal collections - *Cyp4f14*$^{+/+}$ and *Cyp4f14*$^{-/-}$ mice fed γT-10 or γT-165 diets were placed in wire bottom polycarbonate metabolic cages in which urine and fecal pellets could be collected separately. Mice were afforded access to food and water, and collections were made over 24-h following a 24-h acclimation period.

Cyp4f14 expression - Total RNA was extracted from flash frozen tissue liver samples (10-30 mg). Tissue samples were homogenized in 600 μL of RLT containing (1% v/v) β-mercaptoethanol using a rotor-stator homogenizer. Homogenized samples were centrifuged at

10,000 rpm for 3 min to remove debris and the supernatants loaded onto QIAshredder spin columns followed by RNA isolation using the RNeasy Mini Kit, including an on-column DNA digestion step. RNA was reverse-transcribed using High Capacity cDNA Reverse Transcription Kit according to manufacturer's instructions. The cDNA levels were detected using Taqman Universal Master Mix using Roche LightCycler 480 II with pre-designed TaqMan Assays for *Cyp4f14* (Mm00491623_m1) and *Cyp3all* (Mm00731567_m1), using Eukaryotic 18s RNA (Hs99999901_s1) as the reference gene. Amplification conditions were as follows: 50˚C, 2 min; 95˚C, 10 min (1 cycle); 95˚C, 15 s; 60˚C, 1 min (40 cycles); 37˚C, 10 s (1 cycle). The percent remaining expression of each target mRNA relative to 18s mRNA was calculated based on the threshold cycle (Ct) as $2^{-\Delta(\Delta Ct)}$, where $\Delta Ct = Ct_{target}-Ct_{18s}$ and $\Delta(\Delta Ct) = \Delta Ct_{het}–\Delta Ct_{wt}$ or $\Delta Ct_{ko}-\Delta Ct_{wt}$.

Microsomal vitamin E-ω-hydroxylase activity - Microsomal vitamin E-ω-hydroxylase activity was assayed using γ-TOH, δ-TOH, α-TOH, and γ-T3 as substrates complexed with BSA as described (7). The reaction system (0.5 ml) consisted of 0.1 M NaP buffer (containing 0.1 mmol/L EDTA, pH 7.4), 1.0 mM NADPH and 25 ug microsomal protein. Substrate concentrations were 80 µmol/L δ-TOH, 80 µmol/L γ-TOH, 250 µmol/L α-TOH, and 20 µmol/L γ-T3 to account for differences in microsomal uptake of each form of vitamin E (*15*). Following incubation at 37˚C for 15 min and 30 min, hydroxylation products were extracted, derivatized, and quantitated by GC-MS as previously described (*15*), using d_9-α-TOH as internal standard. Product formation for all substrates was linear over the 0 to 30 minute period, the slope of which was used to compare enzyme activity between treatments.

Urine and fecal analysis of tocopherols and metabolites - 24-h urine and fecal samples from *Cyp4f14*$^{+/+}$ and *Cyp4f14*$^{-/-}$ mice fed the γT-10 diet (n=4) and mice fed the γT-165 diet (n=6)

were incubated with β-glucuronidase (800 units for urine, 1600 units for feces dissolved in NaP buffer, pH 6.8) and sulfatase (0.4 units for urine, 0.8 units for feces) for 2 hours at 37˚C. Samples were acidified to pH 2 with 3 N hydrochloric acid (HCl), extracted with hexane-MTBE (3:1), and derivatized as above. Tocopherols and their metabolites were quantified by GC-MS using d_9-α-TOH and d_9-α-CEHC as internal standards.

Tocopherol quantification in tissue and plasma - Solid tissue samples were homogenized in 1 ml 0.9% NaCl, 2 ml of isopropanol and 1 ml MTBE using a Polytron homogenizer, after which 3 ml hexane was added and the mixture shaken then centrifuged to separate organic and aqueous layers. The organic layer was evaporated to dryness using N_2 gas and derivatized as described above. Plasma (40 μL) was extracted with 80 uL ethanol, 100 uL MTBE and 1 ml of hexane. Tocopherols were quantified using GC-MS with d_9-α-TOH as internal standard.

GC-MS quantification of tocopherols and metabolites - A Hewlett-Packard 6890 gas chromatograph (GC) coupled to a Hewlett-Packard 5872 mass selective (MS) detector, operated in selected ion mode, was used for quantification of the various forms of vitamin E and their metabolites. The gas chromatograph was fitted with a Hewlett-Packard HP-1 methylsiloxane capillary column (30 m x 0.25 μm) and operated in split injection mode using helium as the carrier gas. Plasma tocopherols and microsomal ω-oxidation metabolites were resolved isothermally at 280˚C. Analysis of diet, tissue, and fecal tocopherols, and urinary and fecal tocopherol metabolites, was conducted using a temperature program of 200˚C for 2 min, ramped to 250˚C at 7˚C/min, held 6 min, then ramped to 280˚C at 25˚C/min, then held for 16 min. Novel 11'-OH and 12'-OH metabolites of γ- and δ-TOH were identified by their mass spectra using the same temperature program with the instrument operated in scan mode.

Statistical analysis - A goodness of fit Chi Squared test was performed to test whether offspring of *Cyp4f14*$^{+/-}$ breeding pairs were produced in a Mendelian ratio. For RT-PCR data, the average 18s-normalized threshold cycle (ΔCt) for each target gene was compared between the wild-type, heterozygote and knockout samples using Wilcoxon 2 group test, which yielded the estimation of ΔΔCt. Due to the small sample size, a non-parametric test followed by a Bonferonni correction for multiple comparisons was used to compare ΔΔCt between genotype groups. Microsomal enzyme activity data (pmol 13'-OH product/min/mg protein) and in vivo total ω-oxidation metabolite excretion (urine + fecal) were log transformed to meet the assumptions of the statistical tests used. Differences in enzyme activity and ω-oxidation metabolite excretion between genotypes were tested using 1-way ANOVA for each tocopherol substrate, with post hoc multiple comparison corrections using a Tukey's correction.

Mean percentage reductions in enzyme activity and total ω-oxidation metabolite excretion were calculated by comparing individual *Cyp4f14*$^{-/-}$ values with the mean *Cyp4f14*$^{+/+}$ value. These percentage reductions were compared between each tocopherol substrate using a non-parametric Wilcoxon 2 group test, followed by Bonferonni correction for multiple comparisons. 24-h urine and fecal metabolite and tocopherol excretion data was log transformed as necessary. Means or transformed means were compared between genotypes using Student's t-test. As necessary, non-transformed data were compared using a non-parametric Wilcoxon 2-group test. Plasma and tissue α-, γ-, and δ-TOH data were log transformed for comparison between genotypes using 1-way ANOVA, using Tukey's post hoc multiple comparison correction when all three genotypes were compared. All tests were two-sided, and a p-value of <0.05 was considered statistically significant. Analyses were performed using JMP version 8 (SAS Institute).

Results

Identification of Cyp4f14 as a murine TOH-ω-hydroxylase - Treatment of mouse liver microsomes with anti-human CYP4F2 antibodies inhibited TOH-ω-hydroxylase activity by 94% compared to control (**Fig. 1. 2A**), indicating that virtually all TOH-ω-hydroxylase activity in mouse liver microsomes resulted from Cyp4f activity. An ortholog search revealed two murine proteins with >80% sequence identity to that of human CYP4F2 protein, namely Cyp4f15 and Cyp4f14. Both genes were reported to be expressed in murine liver (*25*). Therefore both genes were amplified from mouse liver cDNA, cloned into a mammalian expression vector, and transfected into COS-7 cells, that exhibit no detectable endogenous TOH-ω-hydroxylase activity. Cell-lines that stably express Cyp4f15 and Cyp4f14 were then selected and propagated. Anti-CYP4F2 Western blotting of the stably-transfected cells showed immunoreactive bands at the expected molecular weight of 58 kDa that was not observed in non-transfected controls (**Fig. 1.2B, insert**). These data confirmed that the selected cell-lines expressed the two Cyp enzymes at similar levels.

Membrane preparations from the stably-transfected cell lines were assayed for TOH-ω-hydroxylase activity. Membranes from COS-7/*Cyp4f14* cells exhibited robust TOH-ω-hydroxylase activity whereas those prepared from COS-7/*Cyp4f15* and non-transfected control cultures did not (**Fig. 1.2B**). In addition, ω-hydroxylase activity in COS-7/*Cyp4f14* cultures exhibited a similar substrate selectivity (δ-TOH > γ-TOH > α-TOH) and inhibition by sesamin (data not shown) as human HepG2 and A549 cells, both of which express CYP4F2 and exhibit TOH-ω-hydroxylase activity (*29, 30*). Based on these findings, we concluded that Cyp4f14 is a murine TOH-ω-hydroxylase and proceeded to examine its function in vivo by targeted disruption of its expression in the mouse.

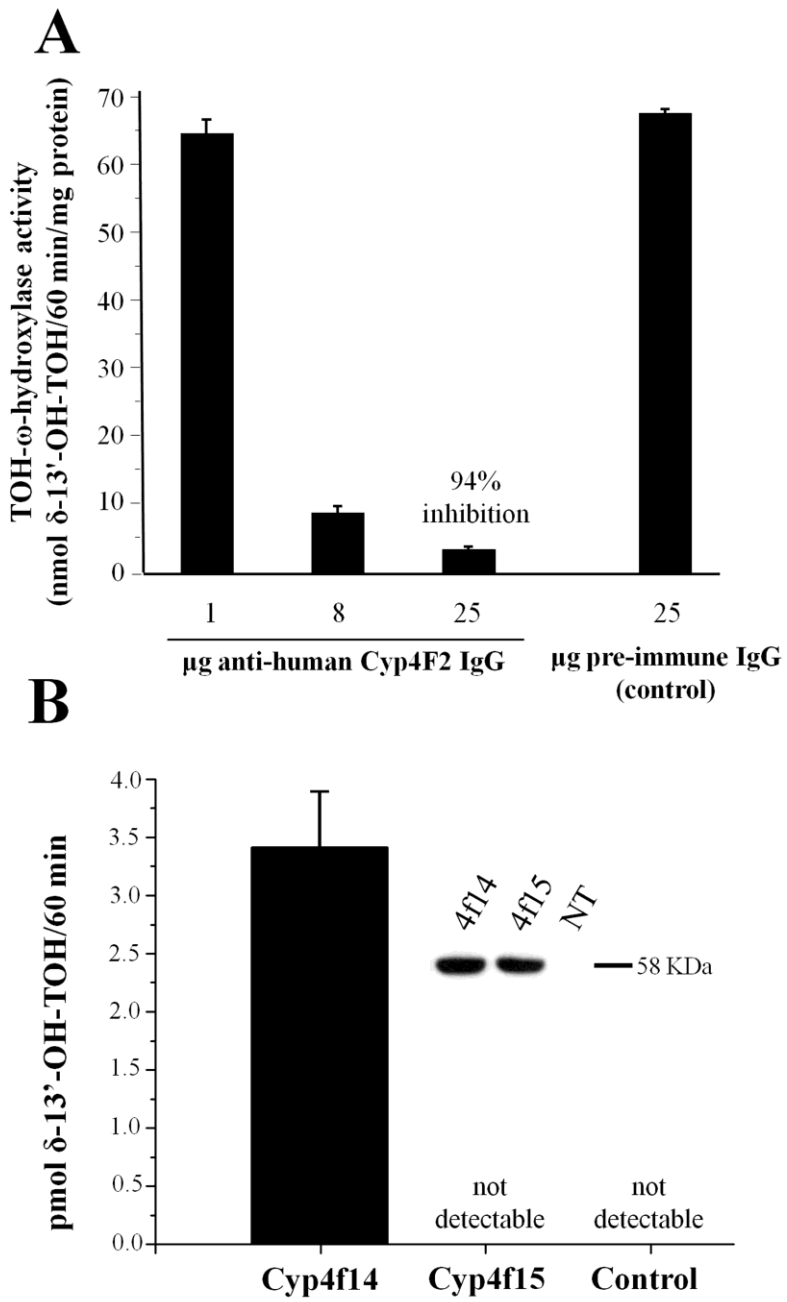

Figure 1.2. Evidence that Cyp4f14 is a functional murine vitamin E ω-hydroxylase. A. **Inhibition of mouse microsomal tocopherol-ω-hydroxylase activity by anti-4F antibody.** Mouse liver microsomes were incubated with indicated concentrations of anti-human CYP4F2 IgG or pre-immune (control) IgG and 60 µM δ-TOH. Formation of 13'-OH-δ-TOH was quantified by GC-MS and normalized to microsomal protein content. **B. Assessment of TOH-ω-hydroxylase activity in COS-7 cell membranes.** Total cell membrane preparations from COS-7 cells expressing Cyp4f14 or Cyp4f15 were incubated with 60 µM δ-TOH, and production of 13'-OH-δ-TOH quantified by GC-MS. The insert shows an anti-CYP4F2 Western blot of the two preparations and of untransfected control (NT).

Generation and Initial Characterization Cyp4f14-disrupted Mice – F1 *Cyp4f14*$^{+/-}$ mice were bred, generating a total of 90 F2 offspring whose genotype segregated in a Mendelian fashion (29% *Cyp4f14*$^{-/-}$, 19% *Cyp4f14*$^{+/+}$, 52% *Cyp4f14*$^{+/-}$). *Cyp4f14*$^{-/-}$ mice exhibited no overt anatomic abnormalities and body weights of the three genotypes were similar irrespective of age or diet. Expression analysis using RT-PCR confirmed the absence of Cyp4f14 mRNA in livers of *Cyp4f14*$^{-/-}$ mice and 50% reduction in *Cyp4f14*$^{+/-}$ mice (**Fig. 1.3B**). Hepatic expression of Cyp3a11 was similar between genotypes in both experimental diet groups (data not shown).

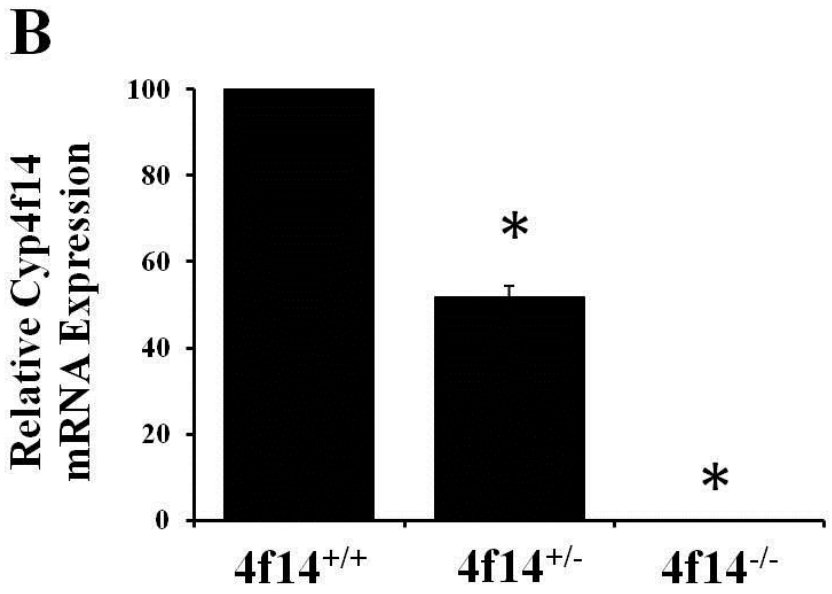

Figure 1.3B. Relative Cyp4f14 mRNA in liver of *Cyp4f14*$^{+/+}$, *Cyp4f14*$^{+/-}$ and *Cyp4f14*$^{-/-}$ mice. Cyp4f14 mRNA in *Cyp4f14*$^{+/-}$ mice was approximately 50 percent of wild-type mice and undetectable in *Cyp4f14*$^{-/-}$ mice ($p<0.05$).

Hepatic vitamin E-ω-hydroxylase activity in Cyp4f14-disrupted mice - Hepatic microsomal vitamin E-ω-hydroxylase activity in mice fed the γT-10 diet was substantially reduced in *Cyp4f14*$^{-/-}$ mice relative to *Cyp4f14*$^{+/+}$ mice. The extent of reduction varied among tocopherol substrates, with the largest reduction seen with γ-TOH (93%); activity

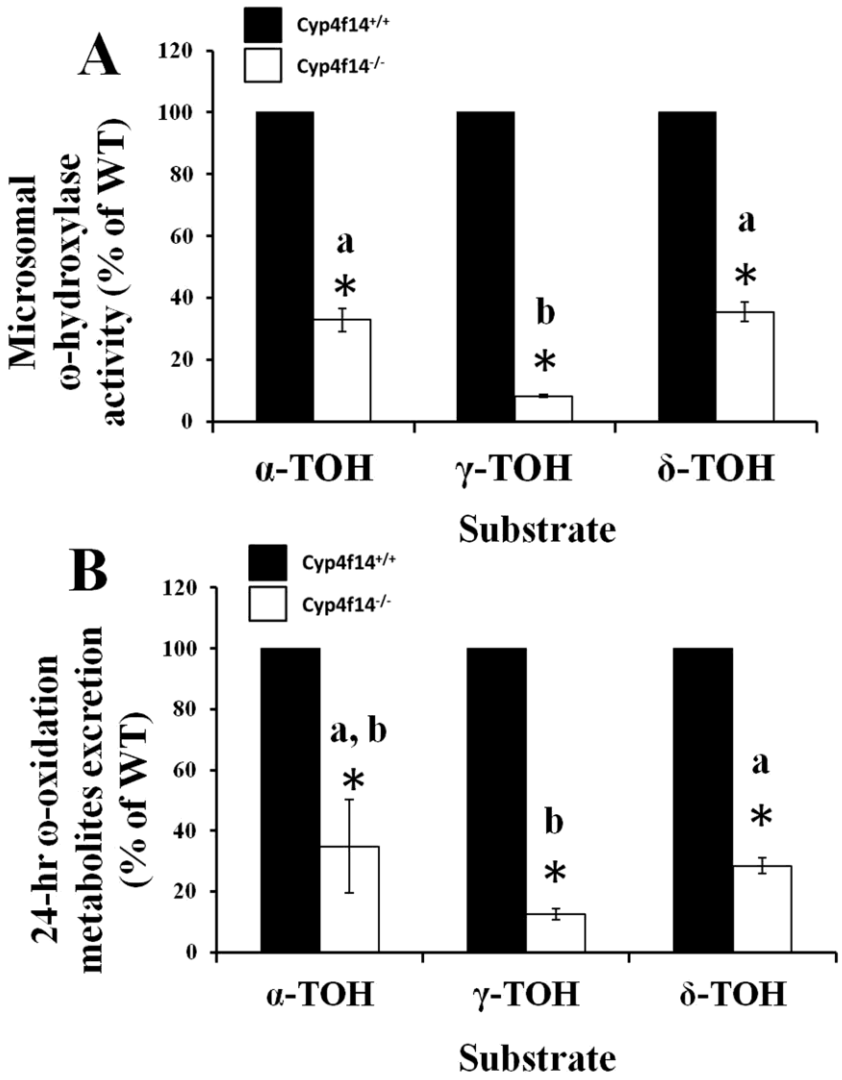

Figure 1.4. Impact of *Cyp4f14* disruption on liver microsomal vitamin E-ω-hydroxylase activity and on whole body excretion of ω-oxidation metabolites (urine + fecal). A. Mouse liver microsomes from wild-type (solid bar) and *Cyp4f14*$^{-/-}$ (open bar) mice fed γT-165 diet were incubated with indicated tocopherol substrates (250 μmol/L α-TOH, 80 μmol/L γ- and δ-TOH) and the corresponding 13'-OH metabolites quantified by GC-MS. Values are percentage of wild-type preparations (n=6). Wild-type activity was 21.0±1.64, 88.1±7.20, and 161.2±11.7 pmol 13'-OH product/min/mg protein toward α-TOH, γ-TOH, and δ-TOH, respectively. Reduction in activity was substrate dependent, with the greatest impact (>90%) on ω-hydroxylation of γ-TOH. Asterisks indicate significant differences from wild-type; different letters indicate significant differences in percent reduction between substrates ($p<0.05$). **B.** 24-Hour urinary plus fecal excretion of total ω-oxidation metabolites (13'-OH, 13'-COOH, and all chain shortened forms) was quantified by GC-MS. Metabolite levels are expressed as percentages of values observed in wild-type mice (n=6). Asterisks represent significant differences from wild-type; different letters indicate significant differences in percent reduction between substrates ($p<0.05$). Wild-type ω-hydroxy metabolite excretion was 0.39±0.10, 109.3±8.82, and 62.5±7.99 nmol/24-hr toward α-TOH, γ-TOH, and δ-TOH, respectively. The pattern of substrate-dependent impact of *Cyp4f14* disruption was similar to that observed in microsomes (A).

toward α- and δ-TOH was 66 and 63% reduced, respectively. ω-Hydroxylation of γ-T3 was reduced by 48% in *Cyp4f14*$^{-/-}$ mice, and reductions in activity in *Cyp4f14*$^{+/-}$ mice were approximately half that of *Cyp4f14*$^{-/-}$ mice (data not shown). Similar results were obtained using microsomes from livers of mice fed the γT-165 diet (**Fig. 1.4A**).

Effect of Cyp4f14 disruption on urinary and fecal excretion of TOH-ω-oxidation metabolites - Metabolic cages were utilized to obtain 24-h urine and fecal samples from *Cyp4f14*$^{+/+}$ and *Cyp4f14*$^{-/-}$ mice. In urine, only short chain metabolites (3'- and 5'-carboxychromanols) of dietary tocopherols were detected. In mice fed the γT-165 diet, urinary excretion of these two γ-TOH metabolites was reduced by about 90% in *Cyp4f14*$^{-/-}$ mice relative to their wild-type counterparts (**Table 1.2**). Smaller but still significant reductions in urinary output of short chain metabolites of α- and δ-TOH were observed in the *Cyp4f14*$^{-/-}$ mice. Similar results were obtained from mice on the γT-10 diet (data not shown).

Table 1.2
24-hr urinary metabolite excretion in Cyp4f14$^{+/+}$ and Cyp4f14$^{-/-}$ mice
Mice were fed the γT-165 diet for six weeks after weaning. Values represent mean ± SEM (n=6).

	Urinary Metabolites§				
	α-3'-COOH	γ-3'-COOH	γ-5'-COOH	δ-3'-COOH	δ-5'-COOH
Cyp4f14$^{+/+}$	0.39 ± 0.10	21.3 ± 2.79	19.9 ± 4.77	23.1 ± 1.47	16.4 ± 3.99
Cyp4f14$^{-/-}$	0.14 ± 0.06*	2.47 ± 0.32*	1.58 ± 0.13*	7.71 ± 1.02*	3.45 ± 0.87*
% Reduction	**65%**	**88%**	**92%**	**67%**	**79%**

§nmol/24 hr
*Significantly different from *Cyp4f14*+/+ mice ($p<0.04$). The 5'-COOH metabolite of α-TOH was not detected.

Table 1.3

24-hr fecal metabolite excretion in Cyp4f14$^{+/+}$ and Cyp4f14$^{-/-}$ mice

Mice were fed the γT-165 diet for six weeks after weaning. Values represent mean ± SEM (n=6).

	Cyp4f14 Genotype	**ω-Hydroxylase Metabolite Products**§							**ω-1, 2 Metabolites**§		**Total Metabolites**§
		3'-COOH	5'-COOH	7'-COOH	9'-COOH	11'-COOH	13'-COOH	13'-OH	11'-OH	12'-OH	
γ-TOH	+/+	6.1 ± 3.1	8.9 ± 2.0	0.9 ± 0.3	15.9 ± 1.9	5.2 ± 0.8	23.4 ± 1.8	7.8 ± 1.0	1.1 ± 0.2	17.6 ± 2.3	86.8 ± 8.0
	-/-	0.8 ± 0.2*	2.5 ± 0.9*	0.2 ± 0.1*	1.7 ± 0.3*	1.7 ± 0.4*	1.6 ± 0.2*	1.2 ± 0.3*	3.3 ± 0.9*	41.3 ± 9.1*	54.2 ± 11.6*
δ-TOH	+/+	2.0 ± 1.3	5.2 ± 2.0	0.3 ± 0.1	2.2 ± 0.4	1.0 ± 0.1	6.5 ± 1.1	5.8 ± 1.0	2.3 ± 0.2	14.9 ± 2.7	37.3 ± 7.4
	-/-	1.1 ± 0.4	2.0 ± 0.4	0.1 ± 0.0	0.5 ± 0.1*	0.4 ± 0.1*	0.5 ± 0.1*	2.1 ± 0.4*	3.2 ± 0.7	17.9 ± 3.0	27.7 ± 4.6

§nmol/24 hr

*Significantly different from *Cyp4f14*+/+ mice ($p<0.05$). Metabolites of α-TOH were undetectable or at trace levels.

Analysis of 24-h fecal samples revealed the presence of all six possible carboxychromanol metabolites and the 13'-OH metabolites of γ- and δ-TOH formed via the ω-oxidation pathway in mice fed the γT-165 diet. Disruption of *Cyp4f14* expression resulted in significant reductions in all seven ω-oxidation metabolites of γ-TOH and the reduction of many δ-TOH metabolites (**Table 1.3**). Fecal levels of δ- and γ-TOH metabolites from mice fed the γT-10 diet were low and similar among genotypes (data not shown). The 13'-OH metabolite of α-TOH was the only appreciable α-TOH metabolite in the feces of both diet groups, and was found at trace concentrations in both genotypes (data not shown).

Whole body 24-h excretion of total tocopherol metabolites generated via the ω-oxidation pathway (urinary plus fecal) in *Cyp4f14*$^{+/+}$ and *Cyp4f14*$^{-/-}$ mice fed the γT-165 diet was calculated. Excretion of ω-oxidation metabolites of the three dietary tocopherols by *Cyp4f14*$^{-/-}$ mice was reduced to approximately the same extents (88, 72, and 65%, respectively for γ-, δ-, and α-TOH) as those observed in the in vitro ω-hydroxylation assays **(Fig. 1.4A-B**).

Fecal excretion of novel ω-1 and ω-2 hydroxylation products of γ- and δ-TOH - Two metabolites not previously reported to occur in vivo, 12'-OH and 11'-OH oxidation products of γ- and δ-TOH, were also observed in fecal samples. The structures of these metabolites were determined by mass spectrometry analysis (**Fig. 1.5**). These represent products of ω-1 and ω-2 hydroxylation activities, respectively. 12'-OH-γ-TOH was the most abundant γ-TOH metabolite in fecal samples of *Cyp4f14*$^{-/-}$ mice fed the γT-165 diet, representing approximately 80% of total fecal γ-TOH metabolites, and was the second most abundant of all excreted γ-TOH metabolites in *Cyp4f14*$^{+/+}$ mice. Interestingly, fecal excretion of 12'-OH-γ-TOH was significantly greater in *Cyp4f14*$^{-/-}$ mice (41.3±9.1 nmol/day) than in *Cyp4f14*$^{+/+}$ mice (7.6±2.3 nmol/day, **Table 1.3**). Consequently, 24-h fecal output of total metabolites (sum of ω, ω-1, ω-2 metabolites of α-, γ-,

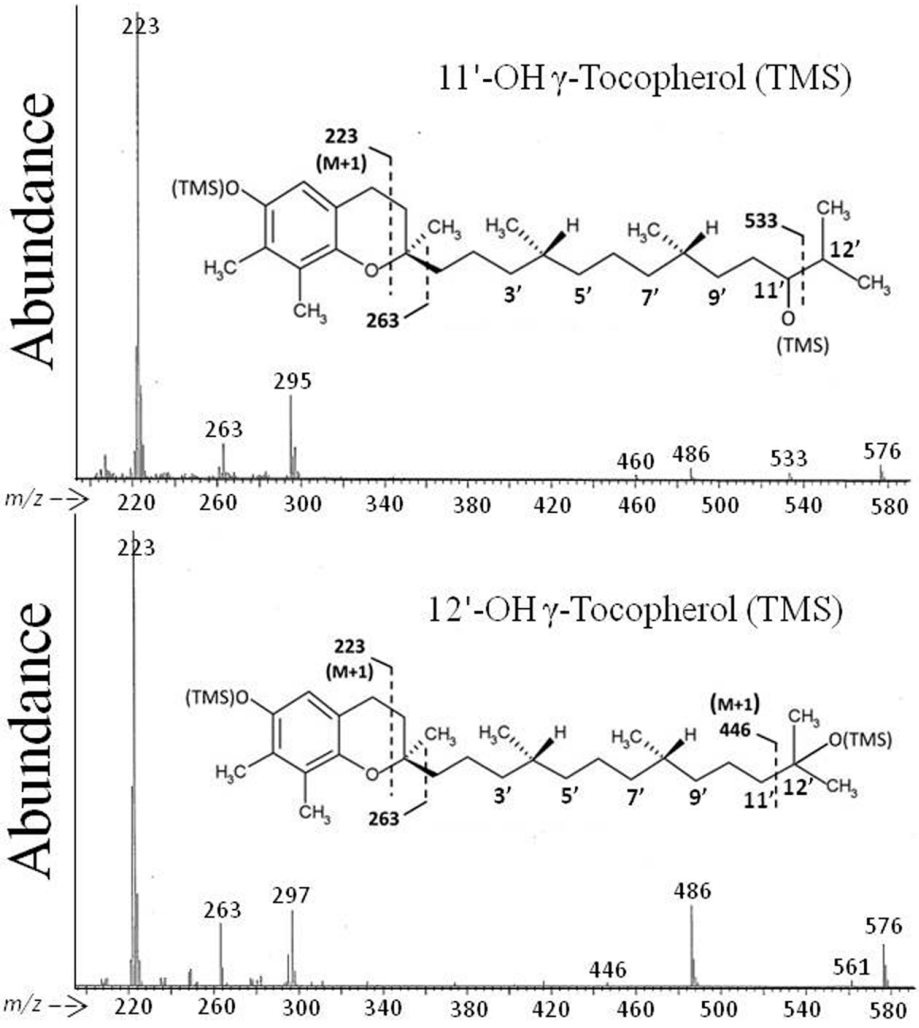

Figure 1.5. Mass spectra of novel fecal ω-1 and ω-2 hydroxy tocopherol metabolites. Lipid extracts of 24-h fecal samples from mice fed a soybean oil diet were derivatized and subjected to electron impact GC-MS analysis. Upper panel: 11'-OH-γ-tocopherol (trimethylsilyl derivative). Lower panel: 12'-OH-γ-tocopherol (trimethylsilyl derivative).

and δ-TOHs) was reduced by only 34% in *Cyp4f14*$^{-/-}$ mice fed the γT-165 diet relative to *Cyp4f14*$^{+/+}$ mice, while the analogous reduction in total urinary metabolites (3'- and 5'-COOH metabolites only) was 81% (**Fig. 1.6A**). In contrast, the excretion of the ω-1 and ω-2

metabolites of δ-TOH was not significantly increased in *Cyp4f14*$^{-/-}$ mice compared to *Cyp4f14*$^{+/+}$ mice (**Fig. 1.6B**).

Fecal excretion of parent tocopherols in Cyp4f14*$^{+/+}$ *and Cyp4f14*$^{-/-}$ *mice - Unmetabolized tocopherols were present in all 24-h fecal samples. In mice fed the γT-165 diet for six weeks, 24-h fecal tocopherol excretion was in the order of γ-TOH>δ-TOH>α-TOH, similar to their prevalence in the diet (**Table 1.1**). Fecal excretion of γ- and δ-TOHs by *Cyp4f14*$^{-/-}$ mice was approximately twice that of *Cyp4f14*$^{+/+}$ mice ($p<0.05$, **Fig. 1.6B**). Fecal excretion of γ-TOH increased from 137 nmol/24-h in wild-type mice to 239 nmol/24-h in *Cyp4f14*$^{-/-}$ mice. The analogous values for δ-TOH were 32 and 63 nmol/24-h in wild-type and *Cyp4f14*$^{-/-}$ mice, respectively.

Effect of Cyp4f14 disruption on plasma and tissue tocopherol concentrations - In *Cyp4f14*$^{-/-}$ mice fed the γT-165 diet for six weeks, concentrations of γ-TOH in plasma and tissues were approximately twice those of *Cyp4f14*$^{+/+}$ mice (**Fig. 1.6C**). In the liver, concentrations of γ-TOH were similar, or in some mice higher, than those of α-TOH. Concentrations of δ-TOH were significantly elevated only in fat tissue, and those of α-TOH were significantly lower in heart tissue (**Table 1.4**). In *Cyp4f14*$^{-/-}$ mice fed the γT-10, liver γ-TOH concentrations, while low, were double those of *Cyp4f14*$^{+/+}$ mice ($p<0.05$); there were no differences between genotypes of concentrations of any tocopherol in other tissues (data not shown).

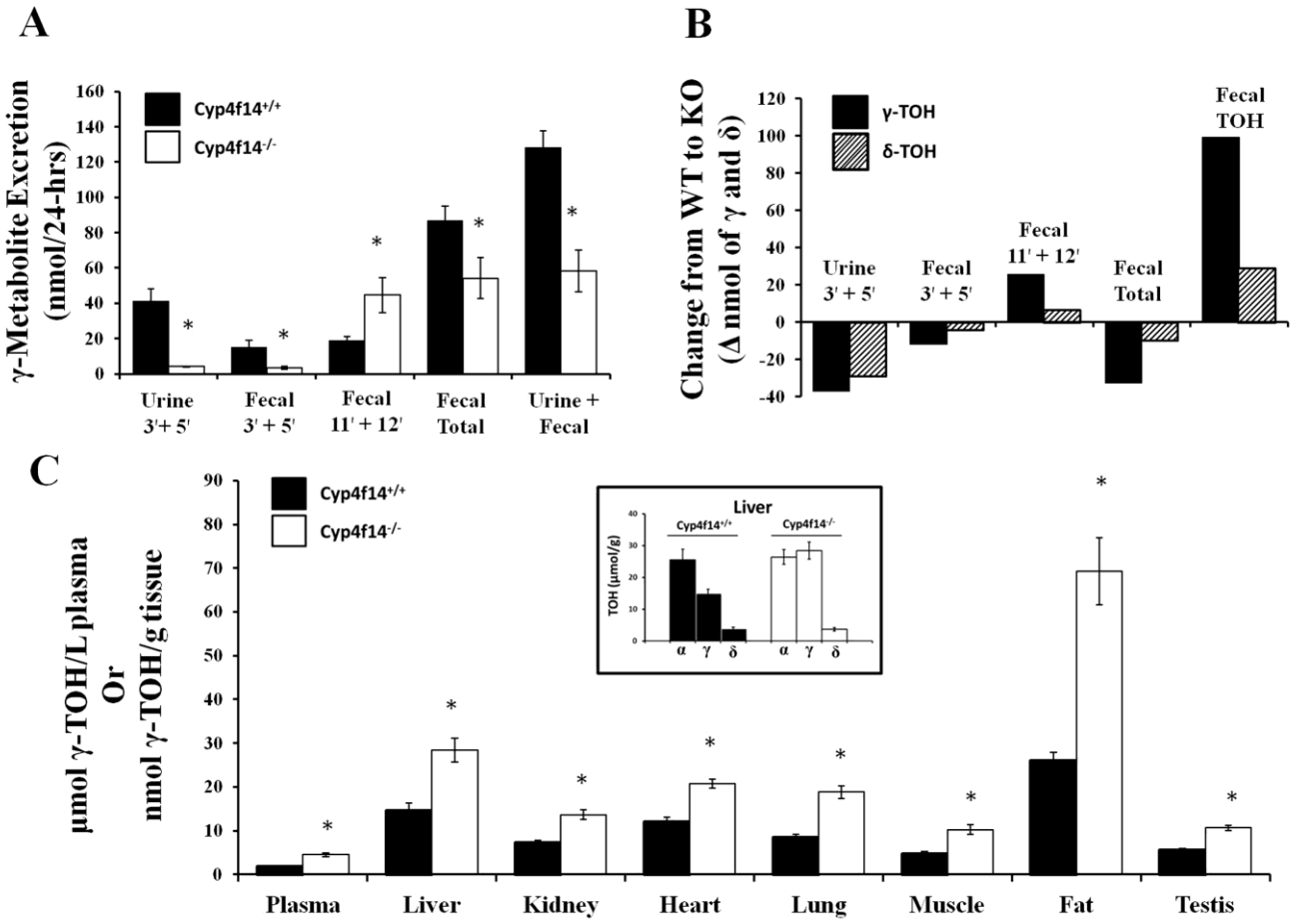

Figure 1.6. Impact of *Cyp4f14* disruption on whole-body TOH metabolism and on concentrations of γ-TOH in plasma and tissues. A. Metabolites of γ-TOH in 24-h urine and fecal collections from wild-type mice (solid bar) and *Cyp4f14*$^{-/-}$ mice (open bar) were quantified by GC-MS. Asterisks indicate significant differences from wild-type mice. **B.** Change (nmol) from wild-type mice to *Cyp4f14*$^{-/-}$ mice in 24 hr urinary and fecal excretion of metabolites of γ-TOH (solid bar) and δ-TOH (hatched bar), or the parent tocopherols. *Cyp4f14*$^{-/-}$ mice counterbalance the loss of ω-oxidation capacity by increased fecal excretion of 11'-OH- and 12'-OH metabolites and parent tocopherols. **C.** Concentration of γ-TOH in plasma and tissues of wild-type (solid bar) and *Cyp4f14*$^{-/-}$ mice (open bar) fed the γT-165 (soybean oil) diet for 6 wks. Insert compares tocopherol composition of liver of wild-type and *Cyp4f14*-null mice. Asterisks indicate significant differences from wild-type mice ($p<0.05$).

Table 1.4

Tocopherol concentration of plasma and tissue of Cyp4f14$^{+/+}$ and Cyp4f14$^{-/-}$ mice

Mice were fed the γT-165 diet for six weeks after weaning.
Values represent mean ± SEM (n=6).

		Tocopherol Concentration		
Tissue	Genotype	α-TOH	γ-TOH	δ-TOH
Plasma	*CYP4f14*$^{+/+}$	8.78 ± 0.34	1.89 ± 0.13	0.36 ± 0.07
	CYP4f14$^{-/-}$	9.55 ± 0.60	4.49 ± 0.39 *	0.45 ± 0.13
Liver	*CYP4f14*$^{+/+}$	25.5 ± 3.27	14.7 ± 1.60	3.64 ± 0.69
	CYP4f14$^{-/-}$	26.4 ± 2.30	28.4 ± 2.75 *	3.70 ± 0.49
Kidney	*CYP4f14*$^{+/+}$	28.4 ± 2.81	7.27 ± 0.50	1.41 ± 0.16
	CYP4f14$^{-/-}$	24.0 ± 1.88	13.7 ± 1.04 *	1.62 ± 0.29
Heart	*CYP4f14*$^{+/+}$	53.6 ± 4.04	12.1 ± 1.06	3.21 ± 0.41
	CYP4f14$^{-/-}$	42.3 ± 1.03 *	20.8 ± 1.07 *	4.44 ± 1.17
Lung	*CYP4f14*$^{+/+}$	41.5 ± 2.54	8.45 ± 0.70	1.49 ± 0.17
	CYP4f14$^{-/-}$	40.0 ± 2.28	18.8 ± 1.37 *	1.90 ± 0.19
Muscle	*CYP4f14*$^{+/+}$	16.7 ± 1.29	4.79 ± 0.39	1.55 ± 0.30
	CYP4f14$^{-/-}$	17.0 ± 1.12	10.3 ± 1.17 *	1.62 ± 0.23
Fat	*CYP4f14*$^{+/+}$	65.6 ± 6.68	26.0 ± 1.98	14.8 ± 1.03
	CYP4f14$^{-/-}$	85.7 ± 8.77	69.2 ± 7.67 *	22.1 ± 3.20
Testis	*CYP4f14*$^{+/+}$	21.6 ± 1.16	5.58 ± 0.40	0.76 ± 0.05
	CYP4f14$^{-/-}$	20.9 ± 1.65	10.6 ± 0.53 *	0.98 ± 0.16

Plasma, μmol/L; tissues, nmol/g.
*Significantly different from *Cyp4f14*+/+ mice ($p<0.02$)

Discussion

Tocopherols and tocotrienols undergo ω-hydroxylation at the terminal methyl groups of their hydrophobic side chains, the first step in their catabolism to short chain carboxychromanols that are excreted in the urine. In the human, TOH-ω-hydroxylation is catalyzed by CYP4F2, which selectively catabolizes forms of vitamin E other than α-TOH. The ω-hydroxylation pathway therefore likely contributes to the α-TOH phenotype, a highly conserved trait in animals. The preferential retention of α-TOH additionally arises from the selection of α-TOH by the tocopherol transfer protein, the absence of which results in severe vitamin E deficiency (*7, 31*). As all forms of vitamin E exhibit similar radical trapping antioxidant activity in vitro (*2*), the evolutionary advantage of the preferential accumulation of α-TOH and the physiological consequences of accumulation of other forms of vitamin E are unknown. In an effort to investigate these issues, we sought to identify the functional murine ortholog of *CYP4F2* and determine the consequences of its deletion on vitamin E metabolism and status.

Cyp4f14, one of 5 functional murine Cyp4f enzymes, exhibited vitamin E-ω-hydroxylase activity when expressed in COS-7 cells. Like CYP4F2, Cyp4f14 is expressed predominantly in the liver. Cyp4f15, a highly homologous murine Cyp also expressed in liver, had no detectable ω-hydroxylase activity. Disruption of *Cyp4f14* by homologous recombination substantially reduced, but did not eliminate, vitamin E-ω-hydroxylase activity in murine liver microsomes. The reduction in activity was substrate dependent, being greatest for γ-TOH (92 percent). These results indicate that at least one other vitamin E-ω-hydroxylase is expressed in the mouse liver. Plasma and tissue tocopherol concentrations in *Cyp4f14*$^{-/-}$ mice fed a diet low in γ- and δ-TOH was similar to those of wild-type mice except for the liver, where γ-TOH levels

were slightly but significantly elevated. However, in mice fed a diet rich in γ-TOH (soybean oil), the metabolic deficit caused by *Cyp4f14* deletion resulted in substantial elevation (2-fold) of γ-TOH concentrations in all tissues and in plasma. Notably, concentrations of γ-TOH in the liver were similar to or higher than those of α-TOH thereby disrupting the α-TOH phenotype in this tissue. Tissue and plasma levels of δ-TOH remained low and unchanged, presumably due to residual δ-TOH-ω-hydroxylase activity sufficient to catabolize the modest amount of δ-TOH in the diet. Accumulation of γ-TOH in *Cyp4f14*$^{-/-}$ mice did not result in any apparent physiologically abnormal phenotype. A 2-3 fold increase in tissue γ-TOH levels significantly reduced protein nitration and ascorbic acid oxidation in an experimental model of inflammation (*32*). Therefore, a model in which non-α-TOH forms of vitamin E accumulate to a greater degree than normal will allow for the investigation of the biological activities of these compounds in regards to disease development, prevention and treatment.

The impact of *Cyp4f14* disruption on whole-body tocopherol metabolism was investigated by analysis of 24-h urine and fecal samples. Urine contained only the shortest chain (3' and 5') carboxychromanol metabolites, while the feces contained the full spectrum of known metabolites of δ- and γ-TOHs formed via the ω-oxidation pathway, with the longer chain metabolites predominating. These results demonstrate that short chain carboxychromanols are directed to secretion from the liver into the bloodstream and filtered by the kidney, while the longer, more hydrophobic metabolites are directed to biliary secretion and excretion via the feces. One major impact of *Cyp4f14* disruption was to dramatically alter the proportion of total metabolites excreted via urinary versus fecal routes. In wild-type mice, 60 percent of total metabolite output was eliminated via the feces, while in *Cyp4f14*$^{-/-}$ mice , in which urinary short chain carboxychromanols were drastically reduced, this proportion rose to 85 percent.

Novel ω-1 (12') and ω-2 (11') hydroxyl metabolites of δ- and γ-TOH were identified in fecal pellets of mice fed the γT-165 diet. These apparently arise in liver and are secreted in bile, as they were detected in the few bile samples able to be obtained from animals fed this diet (data not shown). The 12'-OH metabolite is a terminal metabolite in that it cannot undergo oxidation to the corresponding 12'-keto form, therefore cannot undergo side chain truncation. The metabolic fate of the 11'-OH form remains uncertain. Since we have been unable to confirm the presence of the corresponding 11'-keto form, we assume that it does not materially contribute to the formation of shorter chain carboxychromanols excreted in either feces or urine. Formation of these novel metabolites constituted a significant alternative pathway of metabolism of γ- and δ-TOHs, increasing from 30 percent of total fecal metabolites in wild-type mice to 80 percent in *Cyp4f14*-null mice.

Fecal excretion of 11'-OH and 12'-OH metabolites of γ- TOH was increased substantially in *Cyp4f14*$^{-/-}$ mice, thereby partially counterbalancing the loss of Cyp4f14 activity. This additionally contributed to the impact of *Cyp4f14* disruption on the shift of tocopherol metabolite excretion from the urinary route to the fecal route, and from short chain metabolites to longer chain metabolites. At present it is not known whether the increase in excretion of these ω-1 and ω-2 metabolites resulted from increased activity of a yet unidentified enzyme, or from increased availability of substrate secondary to the loss of Cyp4f14. This increase apparently did not involve the induction of Cyp3a11 since its expression was not altered by disruption of *Cyp4f14*. *Cyp4f14*$^{-/-}$ mice also exhibited increased fecal excretion of parent δ- and γ-TOHs, representing a second means of counterbalancing for the decrement in catabolic capacity. Whether this results from decreased intestinal absorption or increased biliary secretion of tocopherols is unknown as few animals presented with sufficient gall bladder bile for collection.

Nevertheless, the combination of these counterbalancing effects was insufficient to prevent substantial tissue accumulation of γ-TOH in mice fed the soybean oil diet.

Given the importance of α-TTP in the trafficking of α-TOH in the liver, we quantified α-TTP expression by Western blotting as a function of both diet and genetic background. α-TTP was visualized by Western blotting using a rabbit polyclonal antibody raised against the full-length human protein, purified from over-expressing *E. coli*. Neither variable influenced hepatic α-TTP expression (data not shown).

These studies revealed the heretofore unappreciated quantitative importance of fecal excretion of tocopherols and tocopherol metabolites as a mechanism for preventing elevation of tocopherol concentrations in serum and tissues. In wild-type mice, up to 80 percent of whole body output of vitamin E (sum of intact tocopherols and their metabolites) occurred via the feces. This value rose to 96 percent in the *Cyp4f14*-null animals. While Zhao et al (*33*) reported the existence of many tocopherol metabolites in feces, to our knowledge there are no reports of the quantitative contribution of the fecal route to vitamin E status. In addition to the novel ω-1 and ω-2 metabolites reported here, this is the first report of the presence of significant amounts of 13'-OH tocopherol metabolites in feces. How these latter metabolites escape further side chain oxidation is unclear, but suggests that yet-unknown mechanisms are present in the liver that direct these long chain metabolites to biliary secretion.

These studies investigated the effects of *Cyp4f14* deletion on vitamin E metabolism from two perspectives*: in vitro* liver microsomal P450-mediated tocopherol hydroxylation and *in vivo* metabolic capacity as measured by 24-h excretion of tocopherol metabolites in urine and feces. The substrate-dependent decrement resulting from *Cyp4f14* deletion was remarkably similar between microsomal and whole-body measurements of tocopherol ω-oxidation (**Fig.**

2.4). This observation indicates that the liver plays a pivotal role in whole-body vitamin E ω-oxidation that can be qualitatively predicted by microsomal ω-hydroxylation activity. Interestingly, only small amounts of the 12'-OH metabolites of γ- and δ-TOHs were produced in the microsomal system (data not shown), while they comprised a major fraction of tocopherol metabolites in vivo. The reason for this discrepancy is presently unknown.

It is unknown whether the redundancy in the catabolic oxidation of vitamin E evident in mice also exists in humans. The human CYP3A4 has been hypothesized to be involved in vitamin E metabolism based on the finding that supplemental dietary α-TOH in mice leads to increased mRNA expression of its putative ortholog, Cyp3a11, but not that of mouse Cyp4f enzymes (*34*). However, evaluation of all of the major human liver CYP enzymes, including CYP3A4, showed that CYP4F2 was the only CYP enzyme to exhibit ω-hydroxylase activity toward vitamin E (*18*). Additionally, conditions expected to alter CYP4F2 activity result in changes in vitamin E status. For example, short term ingestion of sesame seeds, which contain sesamin, an inhibitor of CYP4F2 (*35*), results in elevation of serum γ-TOH (*36*). A recent genome-wide association study reported that the V433M variant of CYP4F2 was positively associated with plasma vitamin E concentration (*37*). We previously reported that this variant exhibited a reduction in enzyme specific activity by 40-60 percent depending on substrate (*38*). Our heterozygous mice, which display a 50 percent reduction in vitamin E-ω-hydroxylase activity, exhibit a 50 percent increase in tissue γ-TOH concentrations. Taken together, these findings suggest the importance of CYP4F2 as a major regulator of vitamin E composition of human plasma and tissues.

In summary, our data demonstrate that Cyp4f14 is the major, but not the only, vitamin E-ω-hydroxylase in mice, and has critical function in regulating body-wide vitamin E status.

Disruption of *Cyp4f14* expression resulted in hyper-accumulation of γ-TOH in plasma and tissues in mice fed a diet similar in tocopherol composition to that consumed by many human populations. This accumulation occurred despite the combined counterbalancing effects of increased fecal excretion of novel ω-1 and ω-2 tocopherol oxidation metabolites and increased fecal excretion of parent tocopherols. Redundancy in vitamin E-ω-hydroxylase activity and the existence of counterbalancing mechanisms implies a fundamental biological advantage of the α-TOH phenotype that remains elusive.

CHAPTER 2

DISRUPTION OF P450-MEDIATED VITAMIN E HYDROXYLASE ACTIVITIES ALTER VITAMIN E STATUS IN TOCOPHEROL SUPPLEMENTED MICE AND REVEAL EXTRA-HEPATIC VITAMIN E METABOLISM

Introduction

Vitamin E, a family of plant-derived lipophilic compounds, consists of tocopherols (TOHs) and tocotrienols (T3s), and is considered to be the most important group of lipophilic antioxidants. These structurally related compounds differ only in the number and placement of methyl groups on the polar head of the molecule and in the presence of double bonds in the side chain. Interestingly, while the typical American diet contains 2-4 times as much γ-TOH as α-TOH (*4, 5*), α-TOH is present in the serum and tissues at levels 5-6 times that of γ-TOH (*6*). This preferential accumulation of α-TOH in tissues, termed the α-TOH phenotype, is widespread in the animal kingdom and occurs despite the fact that all forms of vitamin E exhibit roughly similar radical scavenging activities (*2, 3*). While *in vitro* and animal studies have suggested both beneficial and detrimental biological actions of non-α-TOH forms of vitamin E, the biological advantage of the α-TOH phenotype remains elusive.

The cytochrome P450 (CYP) superfamily of enzymes catalyze a vast number of catalytic reactions, including the metabolism of lipids, steroids, and xenobiotics. These endoplasmic reticulum-bound enzymes require NADPH and the co-enzyme cytochrome P450 reductase (CPR) for the source and transfer of electrons to the CYP enzyme. We previously identified cytochrome P450 4F2 (CYP4F2) as a human vitamin E-ω-hydroxylase (*18*), catalyzing the hydroxylation of one of the terminal methyl groups of the hydrophobic side chain. This ω-hydroxylation can be followed by oxidation to the corresponding carboxyl form, and a series of

side-chain shortening steps ultimately leading to the formation of the 3' and 5' carboxychromanol metabolites that can be excreted in the urine (*19-21*). CYP4F2 displays substrate preference, such that non-α-TOH forms of vitamin E are metabolized to a greater extent than α-TOH, thereby contributing to the α-TOH phenotype (*15*).

Using a novel *Cyp4f14* knockout mouse model, we have recently identified CYP4F14 as the major mouse vitamin E-ω-hydroxylase, accounting for 70-90% of whole-body ω-hydroxy metabolite production (*39*). This result demonstrated the existence of other vitamin E-ω-hydroxylase enzyme(s) in the mouse. In addition, two novel metabolites were discovered: 12'- and 11'-OH fecal metabolites of δ- and γ-TOH, which are products of ω-1 and ω-2 hydroxylation activities. Interestingly, *Cyp4f14*$^{-/-}$ mice display increased fecal excretion of these novel metabolites as well as increased fecal excretion of unmetabolized TOHs. Despite these counterbalancing effects and redundancy in the TOH-ω-hydroxylase pathway, *Cyp4f14*-null mice fed a modest amount of γ-TOH in the form of soybean oil accumulated 2-fold more γ-TOH than wild-type mice. While the urine has been commonly believed to be the site of TOH metabolites, we found the feces to be the predominant route of metabolite excretion.

The aim of the current work was to investigate whether dietary supplementation with high levels of γ- and δ-TOHs would overcome the counterbalancing effects and result in tissue enrichment above that seen with the previous soybean oil diet. Two experimental models were employed. Firstly, we hypothesized that supplementation with elevated levels γ- and δ-TOH would exacerbate the effect of C*yp4f14* disruption on the tissue accumulation of those TOHs. Secondly, we hypothesized that γ- and δ-TOH supplementation in mice lacking liver-CPR, and therefore all hepatic TOH-hydroxylase activity, would hyper-accumulate TOHs to a greater extent than *Cyp4f14*$^{-/-}$ mice. This model also allowed for the opportunity to determine whether

tissues other than the liver possess this activity. Additionally, we extended the previous findings concerning novel hydroxylase activities to determine their relevance in humans.

Experimental Procedures

Materials - Modified AIN-93G rodent diets were manufactured by DYETS (Bethlehem, PA). Tocopherols were obtained from Matreya, LLC (Pleasant Gap, PA). Bovine serum albumin, NADPH, β-glucuronidase (from *Escherichia coli*), and sulfatase (from *Aerobacter aerogenes*), protease inhibitor cocktail (catalog number P2714), PMSF, EDTA, and glycerol were purchased from Sigma-Aldrich (St. Louis, MO). Pooled human liver microsomes and pooled human small intestine mucosal microsomes were purchased from BD Biosciences (San Jose, CA). The internal standards d_9-α-TOH and d_9-α-CEHC were custom synthesized by J. Swanson (Cornell University, Ithaca, NY).

Tocopherol metabolism and tissue accumulation in *Cyp4f14*$^{-/-}$ mice supplemented with γ- and δ-TOHs - *Cyp4f14*$^{-/-}$ mice, which are viable and fertile, and their wild-type littermates, were generated as described previously (*39*). At 21 days of age, six mice of each genotype (3 male and 3 female) were weaned onto a modified AIN-93G semipufied diet containing 12 mg/kg α-TOH and supplemented with 800 mg/kg each δ-TOH and γ-TOH. After 12 weeks, 24-hr urine and fecal collections were made as described below. Mice were deeply anesthetized by isoflurane inhalation and exsanguinated via cardiac puncture. If bile was present in the gallbladder, it was collected with a syringe and frozen at -80°C until analysis. Heparinized blood was centrifuged at 6,000 x g for 5 min, and serum frozen at -80°C until analysis. Liver, kidney, lung, heart, abdominal fat, and brain tissue samples were flash frozen in liquid nitrogen for vitamin E quantification by GC-MS as described previously (*39*).

Tocopherol metabolism and tissue accumulation in liver-specific *Cpr*$^{-/-}$ mice supplemented with γ- and δ-TOHs - L-*Cpr*$^{-/-}$mice, which have trace liver CYP activity by 2 months of age, and their wild-type littermates, were generated as described previously (*40*). At 2.5 month of age, four male mice of each genotype were fed a modified AIN-93G semipurified diet containing 12 mg/kg α-TOH and supplemented with 800 mg/kg each δ-TOH and γ-TOH. After 4 weeks, 24-hr urine and fecal collections were made as described below. Mice were then euthanized and plasma and several tissues were collected as described above. Approximately 0.6 g of fresh liver was immediately used for preparation of microsomes as described below.

24-Hour urine and fecal collections - Mice were placed individually in wire bottom polycarbonate cages in which urine and fecal pellets were collected separately. Mice were afforded access to food and water, and collections were made over 24-hr following a 24-hr acclimation period.

Liver microsome preparation – Microsomes were prepared from fresh mouse liver by standard differential centrifugation as previously described, resuspended in 0.1 M sodium phosphate (NaP) buffer containing 1 mM EDTA and frozen at -80˚C (*39*). Microsomal protein concentrations were determined by a Bradford-based Bio-Rad assay using bovine serum albumin (BSA) as the standard.

Intestinal mucosa microsome preparation – Mice were euthanized by isoflurane exposure, and upper 12 cm of the small intestine was immediately excised and placed on an ice cold sheet of glass. The removed piece was immediately flushed with ice cold wash buffer (0.9% NaCl containing 1 mM EDTA and 1 mM PMSF), then cut longitudinally, opened, and rinsed with ice cold wash buffer to remove intestinal contents. The mucosal cells were gently scraped off with a razor blade. The intestinal mucosal cells were homogenized using a

Teflon/glass homogenizer with ice cold homogenization buffer (50 mM tris-HCl, pH = 7.4 containing 150 mM KCl, 1 mM EDTA, 20% glycerol, 1 mM PMSF, and 10% protease inhibitor cocktail) and centrifuged at 10,000 x g for 20 min at 4°C. The supernatant was centrifuged at 100,000 x g for 1 h at 4°C. The microsomal pellet was resuspended in 0.1 M NaP buffer containing 1 mM EDTA and frozen at -80˚C. Microsomal protein concentration was determined by a Bradford-based Bio-Rad assay.

Microsomal vitamin-E-ω-hydroxylase activity in L-*Cpr*$^{+/+}$ and L-*Cpr*$^{-/-}$ – Microsomes from mouse liver and small intestine mucosa were assayed for ω-hydroxylase activity using γ-TOH, δ-TOH, and α-TOH as substrates complexed with BSA as described (*15*). The reaction system (0.5 mL) consisted of 0.1 M NaP buffer (pH=7.4), 1.0 mM NADPH and 100 μg microsomal protein. Substrate concentrations were 80 μmol/L for γ- and δ-TOH and 250 μmol/L for α-TOH to account for differences in microsomal uptake of each form of vitamin E (*15*). Following incubation at 37°C for 1 h, hydroxylation products were extracted, derivatized, and quantified by GC-MS as previously described (*15*), using d_9-α-TOH as internal standard.

Analysis of TOHs and metabolites in 24-hr urine and fecal samples – 24-hr fecal collections were homogenized in PBS and an aliquot was used for analysis. Urine and fecal samples were incubated with β-glucuronidase (800 units for urine or 1600 units for feces, dissolved in NaP buffer, pH 6.8) and sulfatase (0.4 units for urine or 0.8 units for feces) for 2 hours at 37°C. Samples were acidified to pH 2, extracted, and derivatized as previously described (*39*). TOHs and their metabolites were quantified by GC-MS using d_9-α-TOH and d_9-α-CEHC as internal standards.

Analysis of bile TOHs and metabolites in *Cyp4f14*$^{+/+}$ and *Cyp4f14*$^{-/-}$ mice - Bile samples from *Cyp4f14* mice (2 wild-type and 3 knockout) were incubated with enzymes (800

units β-glucuronidase, 0.4 units sulfatase) for 2 hours at 37°C. Samples were then acidified and extracted as described above for urine.

Detection of TOH metabolites in human fecal material – Reference fecal material was obtained from an individual following 7 days supplementation of either γ-TOH or α-TOH (400 mg/kg/day). Fecal materials were processed and analyzed for TOH metabolites as described above for mouse fecal samples.

Vitamin E-ω-hydroxylase activity of human liver and intestinal microsomes – Pooled human liver microsomes (HLM) and pooled human intestinal mucosa microsmes (HIM) assayed for vitamin E-ω-hydroxylase activity using γ-TOH (80 μM), δ-TOH (80μM) and α-TOH (250μM) as substrates. The reaction system (0.5 mL) consisted of 0.1 M NaP buffer containing 0.1 mM EDTA, pH 7.4, 2.0 mM NADPH and 200 μg microsomal protein. Following incubation at 37°C for 1 hr, reaction products were extracted, derivatized, and quantified by GC-MS as described above.

Statistical Analysis - All tocopherols and tocopherol metabolites were log transformed as necessary and means were compared between wild-type and knockout mice using Student's t-test. Additionally, tissue TOH concentrations in *Cyp4f14*$^{-/-}$ mice were compared using a two-way ANOVA with genotype and gender as main effects, as well as the interaction effect. When the interaction effect was not significant, it was removed from the model. All tests were two-sided, and a p-value of <0.05 was considered statistically significant. Analyses were performed using JMP version 8 (SAS Institute).

Results

Effect of *Cyp4f14* disruption on 24-hr TOH and TOH metabolite excretion – Metabolic cages were utilized to obtain 24-hr urine and fecal samples from *Cyp4f14*$^{+/+}$ and

Cyp4f14$^{-/-}$ mice fed 800mg/kg of both δ- and γ-TOH for 12 weeks. In urine, only 3'- and 5'-carboxychromanol metabolites of δ- and γ-TOH were detected. Urinary metabolites of γ-TOH were reduced by 88% and those of δ-TOH were reduced by 77% in *Cyp4f14*$^{-/-}$ mice compared to their wild-type littermates. Total urinary tocopherol metabolites were reduced by 82% in *Cyp4f14*$^{-/-}$ mice (**Table 2.1**).

Table 2.1
24-hr urinary metabolite excretion in Cyp4f14$^{+/+}$ and Cyp4f14$^{-/-}$ mice supplemented with γ- and δ-TOH.
Mice were fed the supplemental diet for 12 weeks after weaning.
Values represent mean ± SEM (n=4).

	Urinary Metabolites§				
	γ-3'-COOH	**γ-5'-COOH**	**δ-3'-COOH**	**δ-5'-COOH**	**Total**
Cyp4f14$^{+/+}$	185.9 ± 114.0	133.3 ± 47.9	232.3 ± 111.7	162.1 ± 54.8	713.6 ± 243.6
Cyp4f14$^{-/-}$	29.3 ± 14.0	9.6 ± 4.8*	60.1 ± 11.7	29.6 ± 15.1	128.6 ± 42.4*
% Reduction	**84%**	**93%**	**74%**	**82%**	**82%**

§nmol/24 hr
*Significantly different from Cyp4f14+/+ mice ($p<0.05$). The 3'- and 5'-COOH metabolites of α-TOH were not detected.

Analysis of 24-hr fecal samples revealed the presence of all six carboxychromanol metabolites, as well as the 13'-OH metabolites of γ- and δ-TOH, formed via the ω-oxidation pathway (**Table 2.2**). The 13'-COOH metabolite was consistently the predominant ω-oxidation metabolite in fecal samples. Total ω-oxidation metabolites of γ-TOH were reduced by 79% and those of δ-TOH by 89% in *Cyp4f14*$^{-/-}$ mice. 12'-OH and 11'-OH metabolites of γ- and δ-TOH were also present, formed via the ω-1 and ω-2 oxidation pathways, respectively. These metabolites were also detected in the limited number of gallbladder bile samples that were collected (data not shown).

Table 2.2

24-hr fecal metabolite excretion in Cyp4f14$^{+/+}$ and Cyp4f14$^{-/-}$ mice supplemented with γ- and δ-TOH.

Mice were fed the supplemental diet for 12 weeks after weaning. Values represent mean ± SEM (n=4).

	Cyp4f14 Genotype	ω-Hydroxylase Metabolite Products§							ω-1, 2 Metabolites§		Total Metabolites§
		3'-COOH	5'-COOH	7'-COOH	9'-COOH	11'-COOH	13'-COOH	13'-OH	11'-OH	12'-OH	
γ-TOH	+/+	4.14 ± 1.81	10.8 ± 3.41	0.29 ± 0.04	11.3 ± 2.17	18.7 ± 4.53	53.6 ± 14.2	28.9 ± 5.20	30.9 ± 2.15	222.0 ± 16.9	380.5 ± 29.1
	-/-	0.55 ± 0.32	1.21 ± 0.37*	0.07 ± 0.02	1.3 ± 0.66*	15.3 ± 4.99	3.1 ± 1.2*	5.7 ± 1.44*	54.6 ± 9.18	347.0 ± 55.8	428.8 ± 70.3
δ-TOH	+/+	5.39 ± 2.79	14.1 ± 4.34	0.35 ± 0.05	4.64 ± 0.44	4.98 ± 0.67	93.1 ± 19.5	12.0 ± 2.22	37.1 ± 3.44	157.6 ± 18.3	329.4 ± 21.9
	-/-	0.92 ± 0.50	1.9 ± 0.45*	0.11 ± 0.02*	0.71 ± 0.16*	2.83 ± 0.48*	3.95 ± 0.89*	3.9 ± 0.95*	50.2 ± 10.9	201.5 ± 37.9	266.1 ± 49.4

§nmol/24 hr

*Significantly different from Cyp4f14+/+ mice ($p<0.05$). Metabolites of α-TOH were undetectable or at trace levels.

24-Hr whole body (urine + fecal) ω-oxidation metabolites of γ- and δ-TOH were reduced by 82% in *Cyp4f14*$^{-/-}$ compared to wild-type mice (**Fig. 2.1A**). The sum of 24-hr ω-1 and ω-2 metabolites of γ- and δ-TOH, while numerically higher in *Cyp4f14*$^{-/-}$ mice (30%), was not statistically altered by the disruption of *Cyp4f14*. As a result, the combination of metabolites from all three pathways was 40% reduced in *Cyp4f14*$^{-/-}$ mice. 24-Hr fecal excretion of unmetabolized TOHs was not statistically different between wild-type and *Cyp4f14*-null mice (**Fig. 2.1B**).

Tissue TOH status of *Cyp4f14*$^{+/+}$ and *Cyp4f14*$^{-/-}$ supplemented with γ- and δ-TOHs – *Cyp4f14*$^{-/-}$ mice displayed significantly higher tissue concentrations of δ-TOH in the plasma, lung, and liver averaging a 70% increase in these tissues compared to wild-type mice. *Cyp4f14*$^{-/-}$ mice also had significantly higher γ-TOH in the plasma, lung, kidney, liver and brain, averaging a 90% increase in these tissues compared to wild-type mice (**Fig. 2.1C**). The tissues with the largest difference from wild-type mice were plasma for δ-TOH (2.2-fold higher than wild-type) and brain for γ-TOH (2.7-fold higher than wild-type). A gender effect was observed for many forms of vitamin E such that females had significantly higher levels of TOHs in several tissues. These gender differences were observed in the plasma (γ-, δ-TOH), lung (α-, γ-, δ-TOH), kidney (γ-, δ-TOH), liver (α-, γ-, δ-TOH), heart (α-TOH), brain (α-, γ-, δ-TOH), and fat (δ-TOH). Except for δ-TOH in the plasma, the interaction effect was not significant, indicating the effect *Cyp4f14* disruption on tissue TOH concentration did not differ by gender.

Effect of liver-specific *Cpr* disruption on liver microsomal TOH-ω-hydroxylase activity and TOH metabolism and excretion – Wild-type mice displayed robust hepatic microsomal ω-hydroxylase activity toward γ-TOH (101 pmol product/min/mg protein) and δ-TOH (125 pmol product/min/mg protein). L-*Cpr*-null mice exhibited no detectable ω-

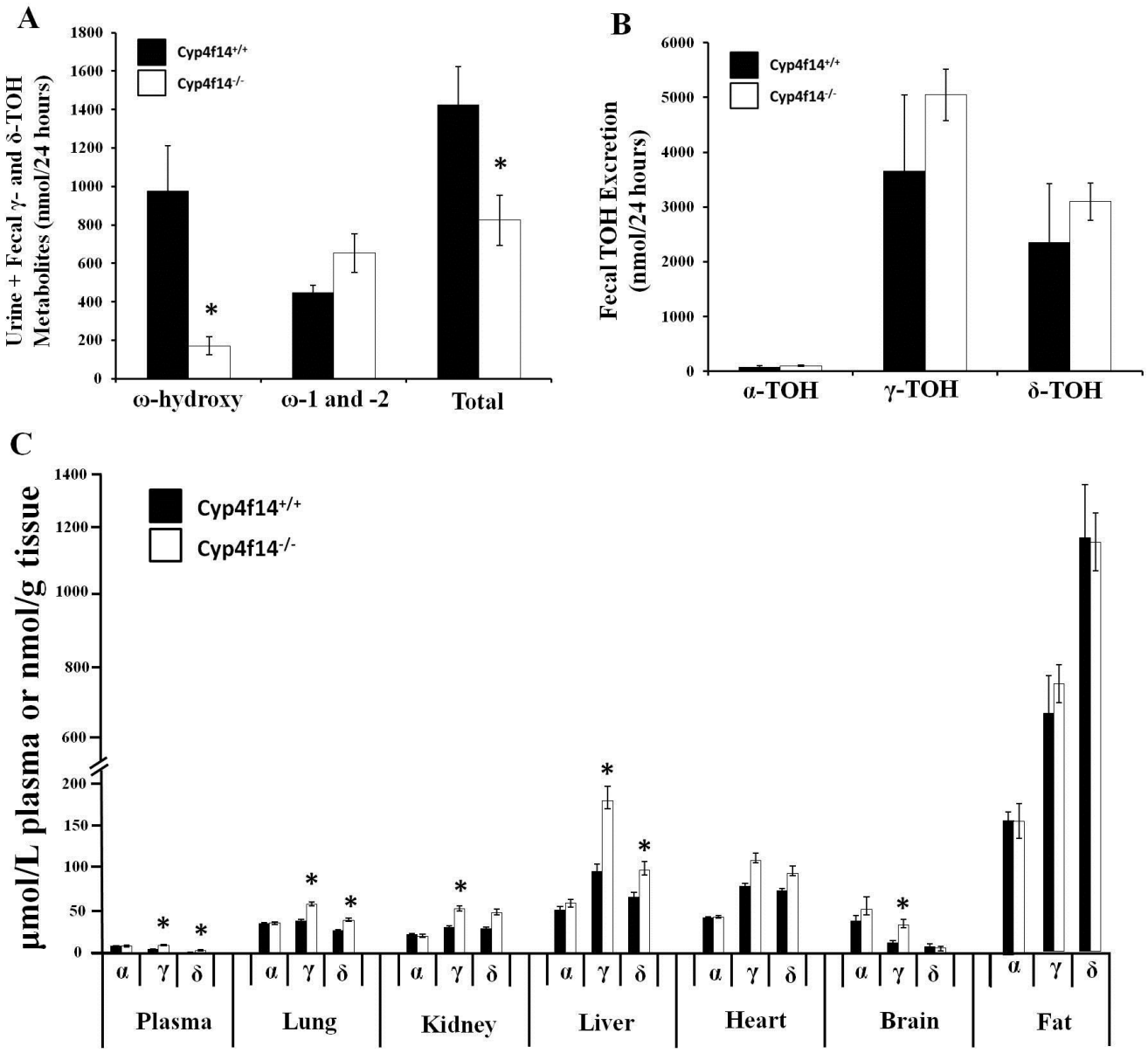

Figure 2.1. Effect of *Cyp4f14* disruption on vitamin E metabolism and tissue accumulation in mice supplemented with γ- and δ-TOH for 12 weeks. A. 24-Hr ω-hydroxy, ω-1/ω-2 hydroxy and total vitamin E metabolite excretion in wild-type (solid bar) and *Cyp4f14*$^{-/-}$ mice (open bar) were quantified by GC-MS. Asterisks indicate significant differences from wild-type. **B.** 24-Hr fecal excretion of unmetabolized TOH in wild-type (solid bar) and *Cyp4f14*$^{-/-}$ mice (open bar). **C.** Concentration of TOHs in plasma and tissues of wild-type (solid bar) and *Cyp4f14*$^{-/-}$ mice (open bar) fed the supplemented diet for 12 weeks. Asterisks indicate significant differences from wild-type mice ($p<0.05$).

hydroxylase activity towards either substrate. Urinary metabolites (3'- and 5'-carboxychromanols) of γ-TOH were reduced by 56% and those of δ-TOH were reduced by 72% in L-*Cpr*$^{-/-}$ mice compared to their wild-type littermates. Total urinary tocopherol metabolites (sum of γ- and δ-TOH metabolites) were reduced by 70% in L-*Cpr*$^{-/-}$ mice (**Table 2.3**). Mice of both genotypes excreted substantially more metabolites of δ-TOH than γ-TOH, despite their similar concentration in the diet. Analysis of 24-hr fecal samples revealed the presence of all previously identified ω-0, ω-1 and ω-2 metabolites of γ- and δ-TOH except 7'-COOH-γ-TOH (**Table 2.4**). As was the case with *Cyp4f14* mice, the 13'-COOH was the predominant ω-oxidation metabolite in fecal samples. 24-Hr whole body (urine + fecal) ω-oxidation metabolites of γ- and δ-TOH were reduced by 70% in in L-*Cpr*$^{-/-}$ mice compared to wild-type mice while ω-1 and ω-2 metabolites were unchanged (**Fig. 2.2A**). The sum of metabolites of both TOHs from all three pathways were 66% lower in L-*Cpr*-null mice. Fecal excretion of unmetabolized TOHs was greater in L-*Cpr*$^{-/-}$ mice compared to wild-type mice for α-TOH (2.4-fold), γ-TOH (3.2-fold), and δ-TOH (6.6-fold; **Fig. 2.2B**).

Table 2.3
24-hr urinary metabolite excretion in L-Cpr$^{+/+}$ and L-Cpr$^{-/-}$ mice supplemented with γ- and δ-TOH.

Mice were fed the supplemental diet for 4 weeks. Values represent mean ± SEM (n=4).

	Urinary Metabolites§				
	γ-3'-COOH	**γ-5'-COOH**	**δ-3'-COOH**	**δ-5'-COOH**	**Total**
L-Cpr$^{+/+}$	43.8 ± 4.49	37.5 ± 3.11	633.3 ± 34.4	56.4 ± 8.74	771.0 ± 43.9
L-Cpr$^{-/-}$	21.5 ± 3.83*	14.0 ± 3.36*	166.5 ± 28.5*	28.3 ± 7.86	230.3 ± 41.3*
% Reduction	**51%**	**63%**	**74%**	**50%**	**70%**

§nmol/24 hr
*Significantly different from *L-Cpr*+/+ mice ($p<0.05$). The 3'- and 5'-COOH metabolites of α-TOH were not detected.

Table 2.4

24-hr fecal metabolite excretion in L-Cpr$^{+/+}$ and L-Cpr$^{-/-}$ mice supplemented with γ- and δ-TOH.

Mice were fed the supplemental diet for 4 weeks. Values represent mean ± SEM (n=4).

	L-Cpr Genotype	**ω-Hydroxylase Metabolite Products§**							**ω-1, 2 Metabolites§**		**Total Metabolites§**
		3'-COOH	5'-COOH	7'-COOH	9'-COOH	11'-COOH	13'-COOH	13'-OH	11'-OH	12'-OH	
γ-TOH	+/+	15.5 ± 8.11	10.9 ± 1.98	ND	4.92 ± 0.96	9.23 ± 2.08	71.1 ± 22.7	19.6 ± 5.38	3.09 ± 0.62	33.5 ± 6.51	167.8 ± 35.7
	-/-	0.79 ± 0.15*	1.74 ± 0.17*	ND	2.84 ± 0.58	7.32 ± 0.58	20.8 ± 2.11*	7.13 ± 1.15	2.62 ± 0.26	23.5 ± 0.80	66.7 ± 3.61*
δ-TOH	+/+	43.8 ± 19.9	39.1 ± 6.74	0.53 ± 0.12	3.73 ± 0.72	4.22 ± 0.99	230.3 ± 61.5	30.8 ± 6.86	12.7 ± 2.17	65.3 ± 16.1	430.3 ± 104.1
	-/-	3.01 ± 1.28 *	4.82 ± 1.06*	0.23 ± 0.08	2.37 ± 0.56	1.74 ± 0.24*	63.6 ± 3.71*	13.5 ± 1.90*	8.67 ± 0.55	65.6 ± 8.46	163.5 ± 4.74*

§nmol/24 hr

*Significantly different from *L-Cpr*+/+ mice ($p<0.05$). Metabolites of α-TOH were undetectable or at trace levels.

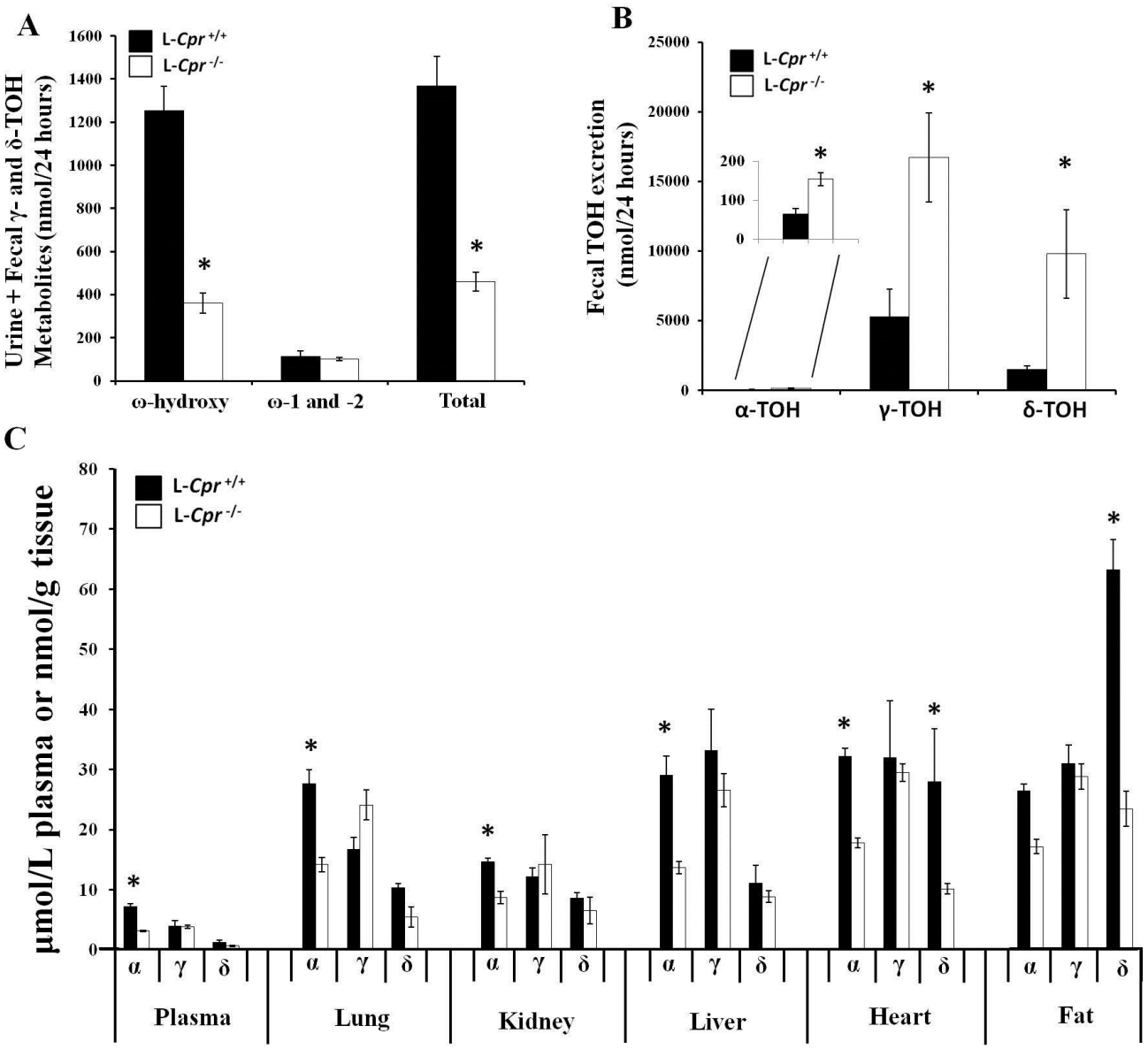

Figure 2.2. Effect of the L-*Cpr* disruption on vitamin E metabolism and tissue accumulation in mice supplement with γ- and δ-TOH for 4 weeks A. 24-Hr ω-hydroxy, ω-1/ω-2 hydroxy and total vitamin E metabolite excretion in wild-type (solid bar) and L-*Cpr*$^{-/-}$ mice (open bar) were quantified by GC-MS. Asterisks indicate significant differences from wild-type. **B.** 24-Hr fecal excretion of unmetabolized TOH in wild-type (solid bar) and L-*Cpr*$^{-/-}$ mice (open bar). **C.** Concentration of TOHs in plasma and tissues of wild-type (solid bar) and L-*Cpr*$^{-/-}$ mice (open bar) fed the supplemented diet for 4 weeks. Asterisks indicate significant differences from L-*Cpr*-null mice ($p<0.05$).

Tissue TOH status of L-*Cpr*$^{+/+}$ and L-*Cpr*$^{-/-}$ supplemented with γ- and δ-TOHs – α-TOH concentrations in L-*Cpr*-null mice were 50% those of wild-type mice in every tissue analyzed (**Fig. 2.2C**). δ-TOH concentrations in the lung, heart, and fat of L-*Cpr*-null mice were, on average, 43% those of wild-type mice. No other significant differences in tissue TOH status between genotypes were observed.

Intestinal musoca microsomal vitamin E-ω-hydroxylase activity in L-Cpr$^{-/-}$ mice – Microsomes prepared from small intestinal musoca of L-*Cpr*$^{+/+}$ and L-*Cpr*$^{-/-}$ mice displayed intestinal vitamin E-ω-hydroxylase activity toward δ-, γ- and α-TOHs. The 13'-OH oxidation products were identified on the basis of retention times, expected molecular ions (562.6, 576.6, and 590.6, respectively), expected fragment ions (209.0, 223.0, 237.0, respectively) and their ratios (**Fig. 2.3**).

TOH-ω-hydroxylase activity in human intestine microsomes and human liver microsomes – HLM and HIM displayed ω-hydroxylase activity toward δ-, γ-, or α-TOH (**Fig. 2.4**). The rank order of activity by substrate for HLM is γ>δ>>α and that for HIM was γ=δ>>α. HIM displayed ω-hydroxylase activity that was 20-30% that of HLM for the three substrates.

TOH metabolites in human fecal material – Fecal material from an individual supplemented with 400 mg/kg/day γ-TOH contained all six γ-carboxychromanol metabolites as well as the 13'-OH, 12'-OH and 11'-OH metabolites. The sum of ω-hydroxy metabolites comprised 80% of total metabolites with the remaining 20% was the 12'-OH and 11-OH metabolites. Fecal material from an individual supplemented with 400 mg/kg/day α-TOH contained the 3', 7', and 11'-α-carboxychromanols and the 13'-OH, 12'-OH and 11'-OH

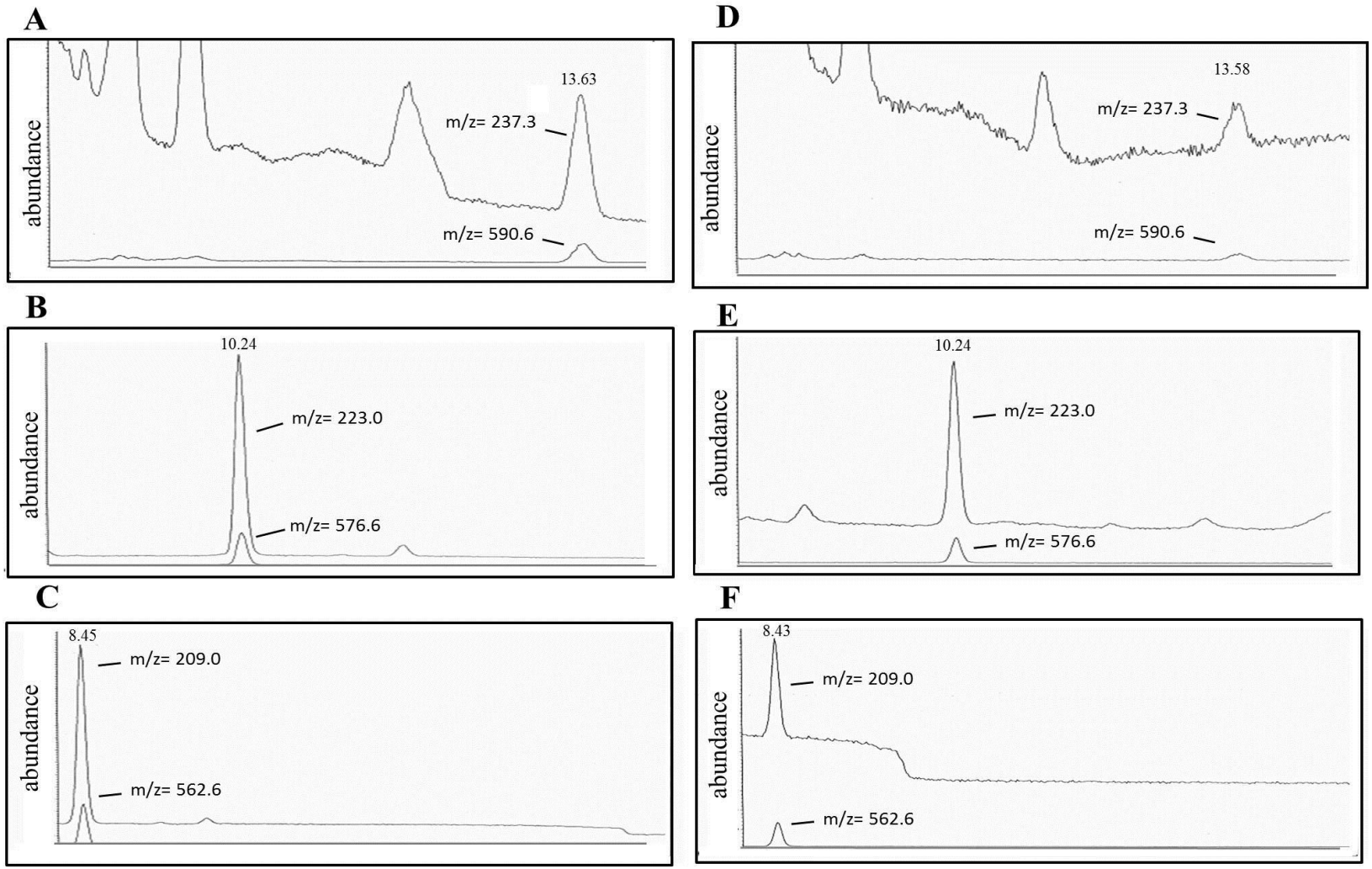

Figure 2.3. Evidence of TOH-ω-hydroxylase activity in microsomes prepared from mouse liver (A, B, C) and small intestinal musoca (D, E, F). GC-MS chromatograms from incubations of liver microsomes with (**A**) 250 μM α-TOH, (**B**) 80 μM γ-TOH, and (**C**) 80μM δ-TOH, illustrating formation of the corresponding 13'-OH metabolites. Microsomes from mouse small intestinal mucosa were incubated with (**D**) 250 μM α-TOH, (**E**) 80 μM γ-TOH, and (**F**) 80μM δ-TOH, illustrating formation of the corresponding 13'-OH metabolites, demonstrating vitamin E-ω-hydroxylase activity in mouse intestine. Retention times and the ratio of the molecular ion to the fragment ion of intestinal samples were consistent with that of the liver.

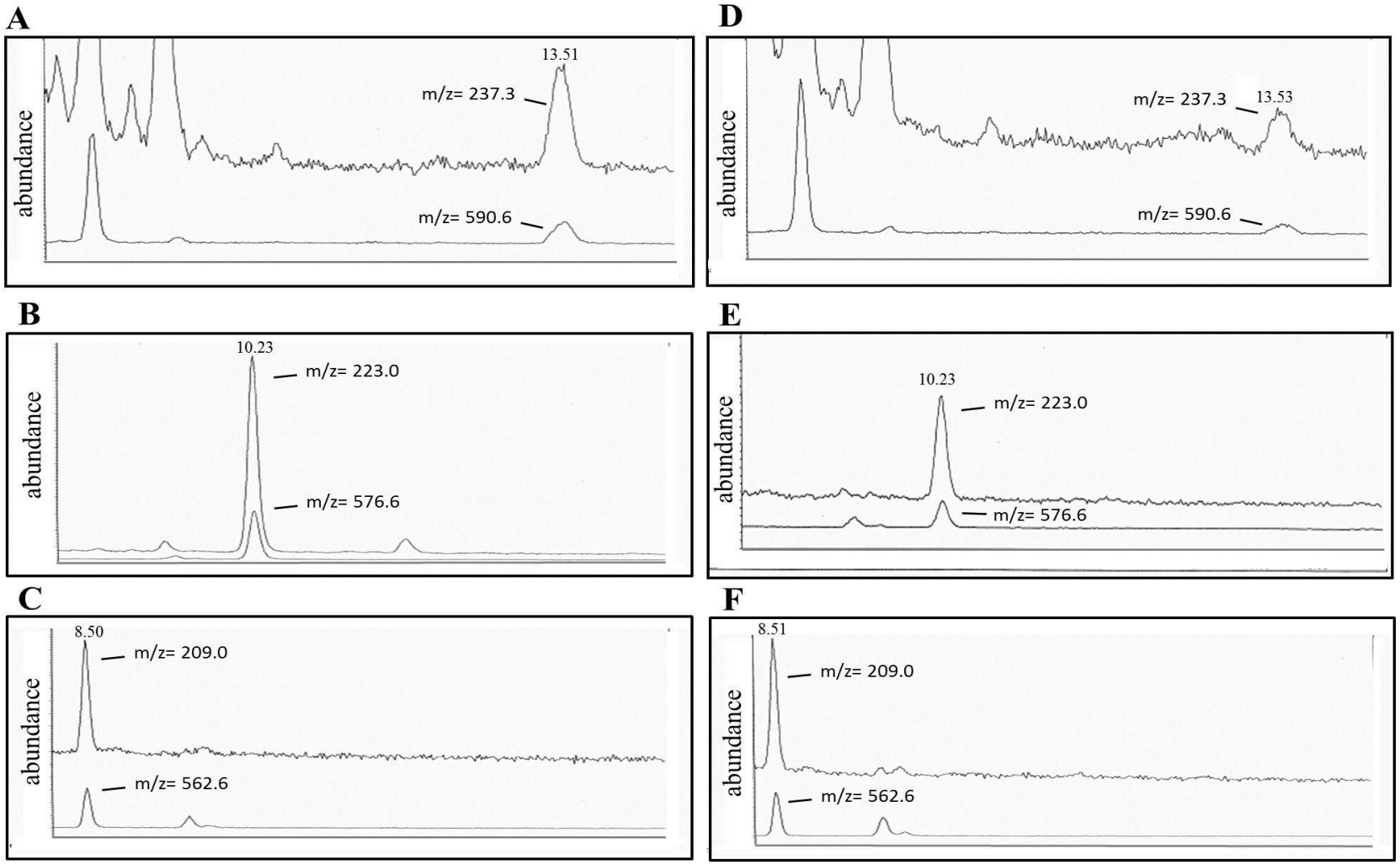

Figure 2.4. TOH-ω-hydroxylase activity in pooled human liver microsomes (A, B, C) and pooled human intestinal microsomes (D, E, F). GC-MS chromatograms from incubations of human liver microsomes with (**A**) 250 μM α-TOH, (**B**) 80 μM γ-TOH, and (**C**) 80μM δ-TOH, illustrating formation of the corresponding 13'-OH metabolites. Human intestinal mucosal microsomes were incubated with (**D**) 250 μM α-TOH, (**E**) 80 μM γ-TOH, and (**F**) 80μM δ-TOH, illustrating the formation of the corresponding 13'-OH metabolites, demonstrating vitamin-E-ω-hydorxylase activity in human intestine. Retention times and the ratio of the molecular ion to the fragment ion of intestinal samples were consistent with that of the liver.

metabolites. ω-hydroxy metabolites represented 30% of total metabolites while the 12'-OH and 11'-OH metabolites comprised the remaining 70%.

Discussion

We previously reported that CYP4F14 is the major vitamin E-ω-hydroxylase in the mouse and that its disruption in mice fed a soybean oil diet containing modest amounts of γ-TOH resulted in elevated tissue levels of γ-TOH relative to wild-type mice (*39*). The accumulation of γ-TOH occurred despite two counterbalancing mechanisms, namely 1) higher excretion of unmetabolized γ-TOH and 2) elevated excretion of novel ω-1 and ω-2 metabolites of γ-TOH. The previous studies also revealed the presence in mice of ω-hydroxylase activity not mediated by CYP4F14. The current work aimed to further characterize the role of vitamin E-ω-hydroxylase in limiting tissue accumulation of TOHs. Specifically, we investigated whether dietary supplementation with high levels of γ- and δ-TOHs would overcome the counterbalancing effects and result in tissue enrichment above that seen with the previous soybean oil diet. Two experimental models were employed: mice with global disruption of *Cyp4f14* and mice with liver-specific disruption of *Cpr* both supplemented with high levels of γ- and δ-TOH.

Supplementation with γ- and δ-TOHs resulted in substantial increases in tissue levels of these forms in both wild-type and knockout mice relative to mice previously fed a soybean oil diet. The increases in tissue levels (7 to 25-fold) were similar or greater than the increase in dietary levels (5-10 fold). While the fold-difference in tissue γ- and δ-TOHs between knockout and wild-type mice was similar to that previously observed in unsupplemented mice, the absolute difference in tissue levels was substantially greater. For example, the effect of *Cyp4f14*

disruption resulted in an increase of 14 nmol/g γ-TOH in the liver of unsupplemented mice, but an increase of 100 nmol/g in liver of supplemented mice, despite being a 2-fold difference between genotypes in both cases. The combination of supplementation and *Cyp4f14* disruption resulted in a 14-fold increase (186 nmol/g) in liver γ-TOH, illustrating the potential of this model to study the biological consequences of tissue enrichment with specific forms of vitamin E.

Interestingly, female mice accumulated significantly more vitamin E in many tissues compared to their male counterparts, irrespective of genotype. Due to the small sample size, statistical analysis of metabolic cage data was not possible, although it does not appear that females metabolize vitamin E to a different extent than males. The reason for this gender effect and its consequences are unknown but warrants further investigation. The dramatic elevation in tissue γ- and δ-TOH occurred in the absence of any overt detrimental effects.

Unlike any other tissue in *Cyp4f14*$^{-/-}$ and wild-type mice, adipose tissue displayed higher levels of δ-TOH compared to γ-TOH, despite similar levels of these forms in the diet. One possible explanation for this finding is that adipose tissue may have vitamin E metabolizing capability such that γ-TOH is being metabolized to a greater extent than δ-TOH. The concentration of δ-TOH was not affected by the disruption of *Cyp4f14*, indicating any vitamin E metabolizing capability in the adipose tissue is through a CYP4F14-independent mechanism. We observed higher levels of unmetabolized fecal γ-TOH than δ-TOH in both *Cyp4f14*$^{-/-}$ and wild-type mice, which could also be contributing to higher δ-TOH levels in adipose tissue.

Cyp4f14 disruption in supplemented mice resulted in substantial loss of whole-body vitamin E-ω-hydroxylase activity (80%), the magnitude of which was similar to that observed unsupplemented mice. While not statistically significant, the higher level of 11'- and 12'-OH metabolites excreted in *Cyp4f14*$^{-/-}$ supplemented mice resulted in attenuation of the overall

metabolic deficit (40%). The counterbalancing effect of these alternative pathways was still an important mechanism in limiting tissue TOH accumulation in the context of supplementation.

Supplemented mice of both gentotypes excreted substantial quantities of unmetabolized TOHs which constituted a significant mechanism of resistant to tissue TOH accumulation. Whether this resulted from decreased intestinal absorption or increased biliary secretion of tocopherols is unknown. In contrast to what is seen in the unsupplemented state, the excretion of unmetabolized TOHs did not constitute a counterbalancing effect in the *Cyp4f14*$^{-/-}$ mice. In the supplemented mice, fecal TOH elimination was a more important means of disposal of dietary TOHs than was metabolic elimination. In wild-type mice fecal TOH elimination was 5 times that of whole-body metabolic disposal, whereas in knockout mice fecal TOH disposal was 10-fold that of metabolic disposal. In this respect, fecal elimination of unmetabolized TOHs served as a high capacity mechanism of resisting tissue accumulation of dietary TOHs under conditions of supplementation. These findings suggest that supplementation was not able to completely overcome the mechanisms of resistance of tissue accumulation constituted by vitamin E metabolism and fecal TOH excretion.

Mice exhibit multiple hepatic TOH-hydroxylase activities in the absence of CYP4F14 that influence diet induced tissue levels of TOHs. Therefore, we utilized L-*Cpr*$^{-/-}$ mice, in which all hepatic CYP activity was absent. If vitamin E metabolizing capacity was restricted to the liver, then these mice should completely lack the ability to metabolize vitamin E. However, in L-*Cpr*$^{-/-}$ mice supplemented with γ- and δ-TOH, whole body metabolic capacity was only reduced by 70%, clearly demonstrating the presence of extra-hepatic ω, ω-1, and ω-2 hydroxylation activities.

Despite significant reductions in vitamin E metabolism in L-*Cpr*$^{-/-}$ mice supplemented with γ- and δ-TOHs, tissue levels of all three TOHs were similar to or actually lower than those of wild-type mice. This finding may have resulted from a reduced efficiency of TOH absorption secondary to the inability to synthesize bile acids. Liver-specific disruption of *Cpr* has been shown to cause 90% reduced bile acid production due to the disruption of CYP7A1 in the liver, the rate-limiting step of neutral bile acid biosynthetic pathway (*41*). This feature additionally complicates the interpretation of the 70% reduction in whole-body in vivo metabolic capacity, and could underestimate the magnitude of extra-hepatic metabolic activity.

We sought to determine potential sites of the vitamin E hydroxylase activities present in L-*Cpr*$^{-/-}$ mice. Since many P450s are expressed in the small intestine, we evaluated that tissue and found ω-hydroxylase activity several forms of vitamin E, although at levels less than that of liver. The contribution of the intestine to whole-body vitamin E metabolic activity is at present unknown but can be investigated using intestine-specific *Cpr* knockout mice. We additionally confirmed the presence of vitamin E hydroxylase activity in human small intestinal mucosa microsomes, validating the mouse as a model to investigate the role of the intestine in first pass vitamin E metabolism.

The ω-1 and ω-2 hydroxylations of δ- and γ-TOH represented quantitative important mechanisms of vitamin E metabolism, accounting for up to 30 percent of whole-body vitamin E metabolites in wild-type mice. The relevance of this finding to human vitamin E metabolism was demonstrated by the identification of all ω-0, ω-1, and ω-2 hydroxy metabolites of γ-TOH in human feces. We additionally identified several fecal ω-hydroxy metabolites and both ω-1 and ω-2 metabolites of α-TOH, the most commonly used form of vitamin E supplement. The enzyme(s) responsible for the ω-1 and ω-2 activities in mice and humans are unknown. The

finding of these metabolites in fecal material raised the possibility that may have arisen from the action of gut microflora. However, this is unlikely since we observed no difference in their concentration in intestinal contents above versus below the cecum (data not shown). Additionally, ceacal samples, with or without a heat treatment sufficient to kill bacteria, were incubated for 24 hrs at 37˚C followed by treatment with deconjugation enzymes. The concentration of ω-1 and ω-2 metabolites was not affected by heat treatment, further supporting the lack of a role of intestinal microflora in the production of these novel metabolites. The presence of these metabolites in the bile of mice indicates that these are likely of hepatic origin.

In summary, supplementation with high levels of γ- and δ-TOH results in tissue enrichment with these forms of vitamin E, and this enrichment is enhanced by the disruption of CYP4F14, the major murine TOH-ω-hydroxylase. However, at these high dietary levels of TOHs, other mechanisms which serve to limit tissue enrichment become more important than the role of the ω-hydroxlyase pathway. These mechanisms consist of the ω-1 and ω-2 hydroxylase pathways and fecal elimination of unmetabolized TOHs, the latter predominating under conditions of supplementation. The use of L-*Cpr*$^{-/-}$ mice, which completely lack all hepatic vitamin E hydroxylase activity, revealed the presence of extra-hepatic vitamin E metabolism in vivo. TOH-ω-hydroxylase activity was observed in the musoca of the small intestine, the first report that a tissue other than the liver is capable of metabolizing vitamin E. These findings were extended to humans with the observations of vitamin E-ω-hydroxylase activity in human intestinal mucosa and fecal excretion of ω-1 and ω-2 metabolites. These findings shed new light on the role of TOH-ω-hydroxlyase activity and other mechanisms in preventing diet induced accumulation of vitamin E in mice and further characterizes vitamin E metabolism in mice and humans.

CHAPTER 3

COMMON VARIANTS OF CYTOCHROME P450 4F2 EXHIBIT ALTERED VITAMIN E-OMEGA HYDROXYLASE SPECIFIC ACTIVITY

Introduction

Cytochrome P450 4F2 (CYP4F2) is an ω-hydroxylase that catalyzes the first step in the only known pathway of vitamin E metabolism, the tocopherol-ω-oxidation (TOH-ω-oxidation) pathway (*14, 18*). CYP4F2 was initially characterized as catalyzing the ω-hydroxylation of leukotriene B4 (LTB4) as well as arachidonic acid (AA) (*42, 43*). The ω-hydroxylation of the terminal methyl group of the phytyl side chain of vitamin E to form the 13'-OH product is followed by the truncation of the molecule into short chain, more water soluble carboxychromanol metabolites that are excreted in urine (*19-21*). Like all CYP enzymes, CYP4F2 is part of an endoplasmic reticulum membrane-bound complex that requires the CYP enzyme itself and reducing equivalents from NADPH via the electron donor cytochrome P450 reductase. While CYP4F2 shares its activity towards AA and LTB4 with several other P450 enzymes, there is no known redundancy in TOH-ω-hydroxylase activity.

Vitamin E is the generic term for several chemical structures including α-,γ-, and δ-tocopherol (TOH) containing a saturated phytyl side chain and having three, two and one methyl group on the chromanol ring, respectively. The corresponding α-,γ-, and δ-tocotrienols (T3) have three double bonds in the phytyl side chain. CYP4F2 exhibits profound substrate preference for non-α-TOH forms of vitamin E (*15*). In addition, the hepatic α-TOH transfer protein (α-TTP) preferentially promotes the secretion of α-TOH from the liver into the bloodstream for transport to tissues (*16*). Together, these two proteins comprise an effective

mechanism that results in the selective accumulation of α-TOH in tissues, and the elimination of other forms of vitamin E, regardless of the relative proportions of each form in the diet (*15*).

Plasma α-TOH concentrations and responses to supplementation in clinical trials vary widely within a healthy population but are consistent within individuals, lending support to the idea that α-TOH status is a genetically determined trait (*44*). Due to the apparent importance of the TOH-ω-oxidation pathway in vitamin E status, it has been suggested that individual single nucleotide polymorphisms (SNP) in the *CYP4F2* gene may contribute to variation in vitamin E status in humans (*45*). Recently, two non-synonymous SNP in the *CYP4F2* gene have been identified: a T to G nucleotide change at mRNA position 84 leading to a tryptophan to glycine substitution at amino acid position 12 (rs3093105; W12G) and a G to A nucleotide change at mRNA position 1347 leading to a valine to methionine substitution at amino acid position 433 (rs2108622; V433M). The W12G variant has a minor allele frequency of 11% and 21% in the European-American and African-American populations examined, respectively, while the V433M variant has a minor allele frequency of 17% and 9%, respectively (*46*). Using a combined Asian sampling panel (Chinese and Japanese HapMap dataset) the minor allele frequency for the W12G variant and the V433M variant are 6% and 26%, respectively (*46*). The existence of the double mutant in humans has yet to be reported. Recently, the V433M polymorphism has been associated with altered warfarin dose requirements in humans (*47*) as well as hypertension (*48*) and ischemic stroke in several populations (*48-50*). Speculative mechanisms behind these associations relate to the role of CYP4F2 in 20-HETE production and the putative role of CYP4F2 as a vitamin K1 oxidase (*51*).

A previous study demonstrated that the V433M substitution in CYP4F2 results in decreased ω-hydroxylation of AA (*46*). The purpose of this study was to determine if the amino

acid substitutions resulting from these two non-synonymous SNP in CYP4F2 cause altered vitamin E-ω-hydroxylase specific activity, using several major dietary forms of vitamin E as substrates.

Materials and Methods

Chemicals and materials. Tocopherols were obtained from Matreya, LLC (Pleasant Gap, PA). The tocotrienols were a gift from Volker Berl (BASF, Ludvigshafen, Germany). Sf9 insect cells were provided by W. Lee Kraus (Cornell University). Insect cell media was purchased from BD Biosciences (San Diego, CA). Insect cell certified fetal bovine serum (BSA) was purchased from Atlanta Biologicals (Lawrenceville, GA) and antibiotic-antimycotic solution was purchased from Mediatech, Inc. (Hemdon, VA). ß-NADPH, hemin chloride, 5-aminolevulinic acid, ferric citrate, and fraction V bovine serum albumin were purchased from Sigma Chemical Co. (St. Louis, MO). The internal standard d_9-α-TOH was custom-synthesized by J. Swanson (Cornell University). Pyridine and N,O-bis-[trimethylsilyl]trifluoracetamide containing 1% trimethylchlorosilane were purchased from Pierce Chemical Co. (Rockford, IL). Insect cell microsomes (BD Supersomes) containing human CYP4F2, cytochrome P450 reductase and cytochrome b_5 were purchased from Gentest (Woburn, MA). PVDF membranes, Odyssey blocking buffer, and IRDye 680 conjugated goat (polyclonal) anti-rabbit IgG were purchased from Li-Cor Biosciences (Lincoln, NE). Rabbit anti-human 4F2 polyclonal antibody was obtained from Fitzerald Industries (Concord, MA). Arachidonic acid and 20-hydroxyeicosatetraenoic acid (20-HETE) were purchased from Cayman Chemical (Ann Arbor, MI).

Generation of baculovirus. Recombinant baculovirus preparations containing four human CYP4F2 enzyme isoforms (wild-type W12/V433, position 12 variant G12/V433, position 433 variant W12/M433, and the double variant G12/M433) were generated by Stec et al as previously described (*46*). The vector contained two promoters that independently drive the expression of CYP4F2 and of the required co-enzyme cytochrome P450 reductase.

Preparation of microsomes containing CYP4F2 variants. Sf9 cells were infected with recombinant baculovirus at multiplicity of infection of 5-10. Sf9 cells were grown in insect cell media with 10% fetal bovine serum and antibiotic-antimycotic solution. At the time of infection, the media was supplemented with hemin (conjugated to bovine serum albumin; 4 μmol/L), 5-aminolevulinic acid (0.5 mmol/L) , and ferric citrate (100 μmol/L). The cells were incubated at 27°C for 3 days following infection. After this time, cells were collected, washed with phosphate buffered saline, resuspended in homogenization buffer (0.1 mol/L sodium phosphate buffer containing 10% glycerol, 1 mmol/L EDTA, 0.1 mmol/L DTT, 1 mmol/L PMSF, pH 7.5) and frozen at -80°C. The cells were then thawed, homogenized using a dounce homogenizer and centrifuged at 10,000 x g for 20 min at 4°C. The supernatant was then subjected to high speed centrifugation at 100,000 x g for 1 h at 4°C. The microsomal pellet was resuspended in 0.1 mol/L sodium phosphate containing 20% glycerol, 1 mmol/L EDTA, 0.1 mmol/L DTT and 0.2 mmol/L PMSF and stored at -80°C. Total microsomal protein concentration was measured using a Bradford-based Bio-Rad assay with BSA as the standard. In addition, negative control Sf9 cells that did not receive virus were prepared in triplicate as described above.

Measurement of CYP4F2 protein. Western blots to quantify recombinant CYP4F2 protein were performed on the microsomes prepared from Sf9 cells. A standard curve of human CYP4F2 (4F2 Supersomes) was run on each gel. The amount of microsomal protein

concentration that was loaded in each lane varied between samples in order to ensure each sample was within the standard curve that was run on each blot. Between 47 and 100 μg of microsomal protein were heated to 95°C for 5 minutes, electrophoresed on 12% SDS-polyacrylamide gels, and blotted onto PVDF membrane. Membranes were blocked with Odyssey blocking buffer for 2 h at room temperature and then incubated with rabbit anti-human 4F2 polyclonal antibody (1:300). The membranes were then incubated with IRDye 680 conjugated goat (polyclonal) anti-rabbit IgG for 1 h at room temperature. The membranes were visualized using an Odyssey infared imager (Li-Cor, Lincoln, NE) with densiometric analysis performed using Odyssey software. The concentration of CYP4F2 protein in the microsomal preparations prepared from each human CYP4F2 variant was derived from the standard curve on each individual blot.

Measurement of vitamin E-ω-hydroxylase activity. A comparison of CYP4F2-dependent vitamin E-ω-hydroxylase activity among the four enzyme isoforms using Sf9 microsomes obtained from three independent transfection batches was first determined using δ-TOH as substrate. The reaction system (0.5 mL) consisted of sodium phosphate (NaP) buffer (0.1 mol/L, with 0.1 mmol/L EDTA, pH=7.4), 60 μmol/L δ-TOH added as a complex with 1% (w/v) fraction V BSA prepared as previously described (*15*), and the volume of each of the four microsomal preparations sufficient to achieve equivalent total microsomal protein concentration. Microsomes were preincubated with the substrate-BSA complex at 37°C for 5 min after which point NADPH was added to a final concentration of 2 mmol/L and the system incubated for 35 min at 37°C. The reaction was terminated and δ-13'-OH-TOH product extracted and derivitized as previously described (*15*). d_9-α-TOH was used as internal standard.

An investigation of the impact of the single and double mutations using several tocopherols (α-, γ-TOH) and tocotrienols (α-, γ-, δ-T3) as substrate was then performed using microsomes from the same transfection batch. Conditions for evaluation of ω-hydroxylation of γ-TOH were similar to that of δ-TOH described above. Those used for assay of metabolism of α-TOH and tocotrienols were similar except for substrate concentrations (α-TOH, 350 μmol/L; tocotrienols, 10 μmol/L) to account for differences in membrane uptake as characterized previously (*15*). In addition, several of these substrates were assayed at a lower concentration (γ-, δ-TOH: 30 μmol/L; α-T3: 4 μmol/L). The analogous 13'-ω-hydroxylated reaction products were extracted and derivatized as described above.

Measurement of arachidonic acid ω-hydroxylation. Assays to determine the AA-ω-hydroxylase specific activity were performed in NaP buffer with 42 μmol/L AA without BSA, and an equal amount of microsomal protein from each of the four microsomal preparations from one transfection batch in 0.5 mL reaction volume. Reaction mixtures were preincubated for 5 min at 37°C after which time NADPH (2 mmol/L) was added and incubations continued for 35 min at 37°C. 20-HETE was extracted and derivatized after acidification as described above, using d_9-α-TOH as internal standard.

GC-MS. A Hewlett-Packard 6890 gas chromatograph, coupled to a Hewlett-Packard 5872 mass selective detector operated in selected ion mode, was used for quantification of vitamin E and AA reaction products. The gas chromatograph was fitted with a Hewlett-Packard HP-1 methylsiloxane capillary column (30 m X 0.25 mm) and operated in split injection mode using helium as the carrier gas. Long-chain TOH and T3 metabolites were resolved isothermally at 280°C for 20 minutes. 20-HETE was resolved using a temperature program starting at 180°C, ramping to 250°C at a rate of 6°/min, then to 280°C at a rate of 25°/min, holding at 280°C for 13

min. Metabolite product was quantified using the d_9-α-TOH internal standard. 20-HETE values were corrected using a relative detector response factor of 50.

Calculation of enzyme specific activity. Enzyme activity data (pmol product/min) were normalized to the microsomal CYP4F2 protein content as determined by quantitative Western blotting to yield specific activity (pmol $\cdot$ min^{-1} $\cdot$ pmol $4F2^{-1}$). Data are presented as specific activity or as percentage of wild-type specific activity.

Statistical analysis. Three independent transfection batches of the four microsomal enzyme isoform preparations were each assayed in triplicate for the initial comparison of specific activities using δ-TOH as substrate. Each of the three batches was analyzed independently using one-way ANOVA. When significant main effects of enzyme isoform were detected, post hoc multiple comparisons were performed using a Tukey correction. The comparison of specific activities of the four enzyme isoforms using various tocopherol and tocotrienol substrates was performed in triplicate using the same transfection batch. In order to assess the effect of enzyme isoform on CYP4F2 specific activity, Student's t-test was used to compare the specific activity of each variant enzyme to that of the wild-type enzyme for each substrate individually. In addition, for each of the three variants, the mean percent of wild-type value for each tocopherol substrate was compared to the mean percent of wild-type value of the other two tocopherol substrates using one-way ANOVA followed by multiple comparisons with a Tukey correction. Similarly, for each of the three variants, the mean percent of wild-type value for each tocotrienol substrate was compared to the mean percent of wild-type value for the other two tocotrienol substrates using one-way ANOVA followed by multiple comparisons with a Tukey's correction. Differences in arachidonic acid-ω-hydroxylase specific activity between the four enzyme isoforms were determined using one-way ANOVA followed by multiple comparisons with a

Tukey's correction. Values in the text are means ± SD. All statistical analyses were performed using JMP version 8 (SAS Institute Inc.). If needed, responses were log-transformed to meet the assumptions of the statistical tests. All tests were 2-sided, and $P < 0.05$ was considered to constitute statistical significance.

Results

Expression of CYP4F2 variants in Sf9 microsomes. A 53-kDA protein that co-migrated with human CYP4F2 standard was observed in each of the four CYP4F2 microsomal preparations (W12/V433 [WT], G12/V433, W12/M433, G12/M433). A representative blot from one of the transfection batch is shown in **Figure 3.1**. Negative control microsomal preparations did not show a band at 53-kDA (**Figure 3.1B**).

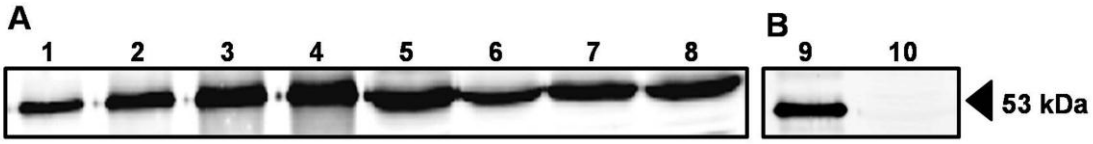

Figure 3.1. CYP4F2 expression of four enzyme isoforms in Sf9 microsomal preparations. Lanes 1-4: CYP4F2 standard of 0.05, 0.10, 0.15 and 0.20 pmoles, respectively. Lanes 5-8, CYP4F2 isoforms: WT, W12G, V433M, W12G/V433M, respectively, (**A)**. Lanes 9 and 10 (from a separate blot): CYP4F2 standard of 0.15 pmoles and negative control microsomes, respectively, (**B)**. Western blotting using antibodies against CYP4F2 detected a 53-kDa protein that co-migrated with CYP4F2 standard. Blots are representative of three independent transfection batches.

δ-TOH ω-hydroxylase specific activity of wild-type and variants of CYP4F2. All assayed microsomal preparations except the negative controls showed production of δ-13'-OH-TOH as determined by electron impact mass spectroscopy. Analysis of log-transformed data from one transfection batch indicated the mean δ-13'-OH-TOH production of wild-type enzyme

was significantly different from the three variants after normalization to microsomal CYP4F2 protein content (**Figure 3.2**). The W12G substitution resulted in significantly higher δ-13'-OH-TOH production (275% of wild-type enzyme, $P < 0.0001$) compared to wild-type. In contrast, the amino acid substitution at position 433 resulted in decreased δ-13'-OH-TOH production (66% of wild-type enzyme, $P < 0.02$). The effect of the double mutation was the same as the single mutation at position 433, exhibiting diminished specific activity (60% of wild-type enzyme, $P < 0.007$). Microsomal preparations from all three transfection batches showed similar differences in specific activity due to the mutations, except that in one batch the activity of the double mutant was not statistically different from that of wild-type (data not shown). The relative enzyme specific activities using 30 μM δ-TOH were consistent with the results observed using 60 μM δ-TOH. The W12G variant exhibited 145% of wild-type enzyme specific activity, while the V433M variant and the double variant exhibited 37% and 66% of wild-type specific activity, respectively, at the lower concentration.

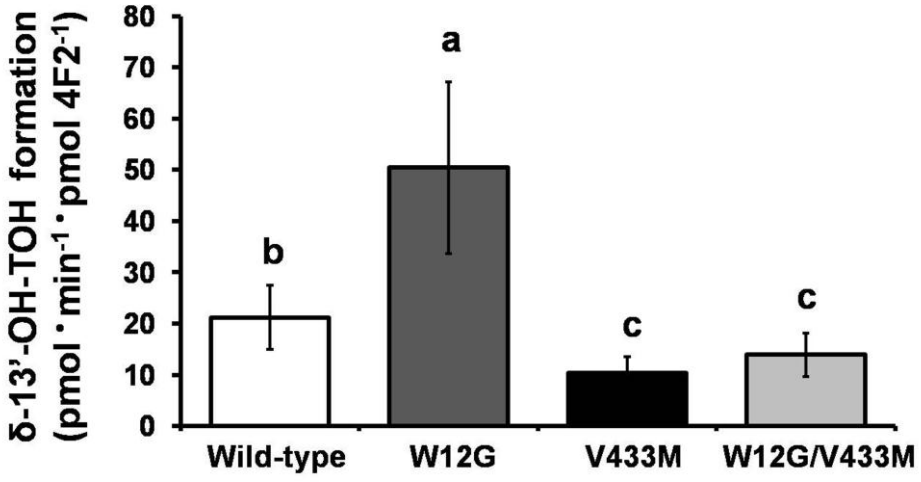

Figure 3.2. δ-TOH-ω-hydroxylase specific activity of CYP4F2 isoforms. δ-13'-OH-TOH formation was determined in microsomal incubations containing 60 μmol/L δ-TOH-BSA complex. Data are means ± SD, n=3. Means without a common letter differ, $P < 0.05$.

Comparative metabolism of various tocopherols and tocotrienols by CYP4F2 variants.

The W12G enzyme variant exhibited significantly greater specific activity toward all three tocopherols tested (255 ± 22 percent of wild-type, $P < 0.0001$, **Figure 3.3A**). In sharp contrast, the V433M enzyme variant exhibited significantly decreased ω-hydroxylase activity toward all three tocopherols (57 ± 14 percent of wild-type, $P < 0.03$, **Figure 3.3B**). Among the tocopherol substrates, α-TOH was the most negatively impacted by the V433M substitution, but was the least impacted by the gain-of-function effect of the W12G substitution. The W12G/V433M double mutant exhibited reduced specific activity toward all three tocopherols, similar to what was observed for the V433M variant (48 ± 14 percent of wild-type, $P < 0.002$, **Figure 3.3C**). The relative specific activities of the enzyme isoforms obtained using 30 μM γ-TOH were consistent with those observed using 60 μM γ -TOH, with the W12G variant resulting in 162% of wild-type specific activity, while the V433M variant and the double variant exhibited 47% and 68% of wild-type specific activity, respectively, at the lower concentration.

As was the case with tocopherol substrates, the W12G variant exhibited much higher specific activities toward all three tocotrienol substrates (353 ± 2 percent of wild-type, $P < 0.003$, **Figure 3.4A**). In contrast, the V433M substitution had little or no effect on specific activity toward the tocotrienols, with a marginally significant difference from wild-type evident with δ-T3 as substrate ($P = 0.046$, **Figure 3.4B**). Again, results of the double mutant were similar to those obtained with the V433M variant (**Figure 3.4C**). In contrast to the case with tocopherols, none of the three variants exhibited significant differences in specific activity among the three tocotrienol substrates. Additionally, the relative specific activities of the enzyme isoforms obtained using 4 μM α-T3 were consistent with those observed using 10 μM α -T3. The W12G

variant exhibited 203% of wild-type specific activity while the V433M variant and the double variant exhibited 84% and 106% of wild-type specific activity at the lower concentration.

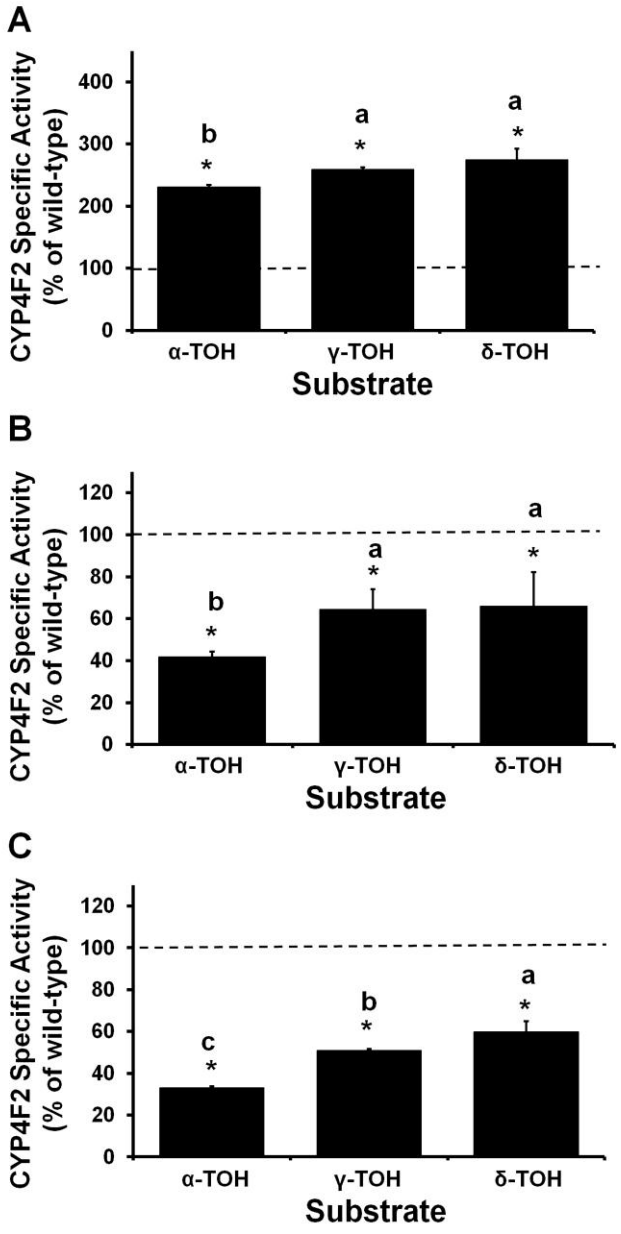

Figure 3.3. Alterations in ω-hydroxylation of tocopherols by CYP4F2 isoforms W12G (A), V433M (B), W12G/V433M (C). Enzyme specific activity (pmol product $\cdot min^{-1} \cdot$ pmol $CYP4F2^{-1}$) for each of the three variants is expressed as percent of the wild-type activity value. Dotted line represents 100%, i.e. wild-type. Data are means ± SD for each tocopherol evaluated, n=3. *different from wild-type, $P < 0.03$. Within each graph, means without a common letter differ, $P < 0.05$.

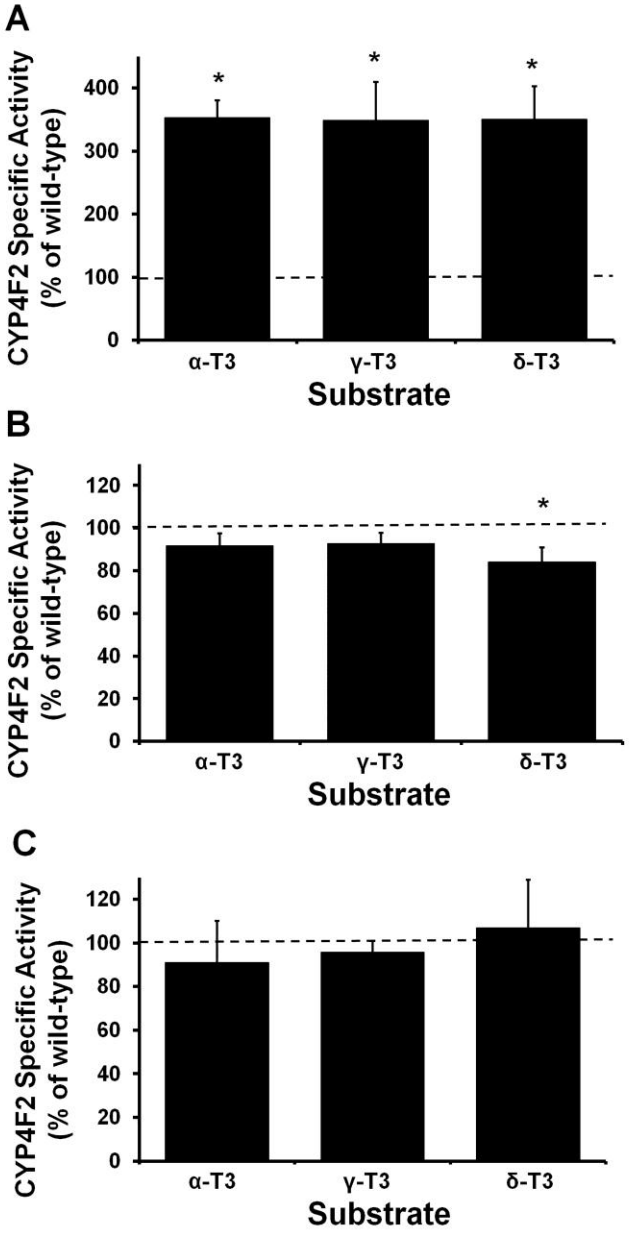

Figure 3.4. Alterations in ω-hydroxylation of tocotrienols by CYP4F2 isoforms W12G (A), V433M (B), W12G/V433M (C). Enzyme specific activity (pmol product $^{\bullet}$ min^{-1} $^{\bullet}$ pmol $CYP4F2^{-1}$) for each variant is expressed as percent of the wild-type activity value. Dotted line represents 100%, i.e. wild-type. Data are means ± SD for each tocotrienol evaluated, n=3. *different from wild-type, $P < 0.05$. Within each graph, no means were significantly different from each other ($P > 0.05$).

ω-Hydroxylation of arachidonic acid by CYP4F2 variants. In light of the finding of a significant gain-of-function effect of the W12G variant on vitamin E metabolism, the four enzyme isoforms were re-evaluated with respect to arachidonic acid ω-hydroxylation. The specific activity of the W12G variant was significantly greater than that of wild-type enzyme (190% of wild-type enzyme, $P < 0.0009$, **Figure 3.5**). The V433M variant exhibited a severe loss-of-function (20% of wild-type enzyme, $P < 0.0009$), an effect similar to the loss-of-function observed with the double mutant (22% of wild-type enzyme, $P < 0.0009$). Thus, the effects of the three variants on ω-hydroxylation of arachidonic acid mirrored the effect of the ω-hydroxylation of the three tocopherols.

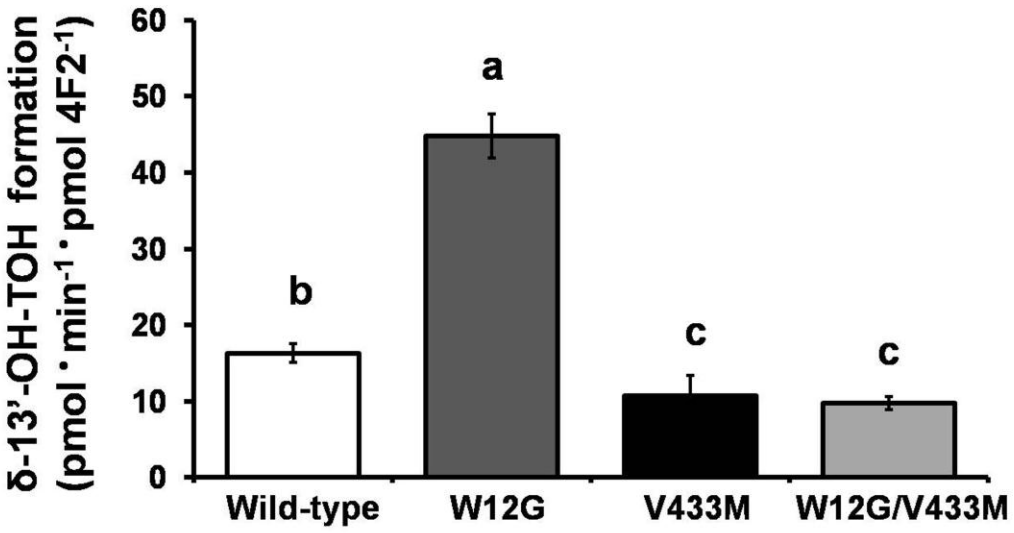

Figure 3.5. Metabolism of arachidonic acid by CYP4F2 isoforms. 20-HETE formation was determined in incubations containing 42 μmol/L AA. Data are means ± SD, n=3. Arachidonate ω-hydroxylase specific activity was compared between the four enzyme isoforms. Means without a common letter differ, $P < 0.05$.

Discussion

CYP4F2 catalyzes the initial step in the only known enzyme-mediated pathway of vitamin E metabolism, the vitamin E-ω-oxidation pathway (*14*). The product of the reaction, the hydroxyl derivative of one of the two terminal methyl groups of the hydrophobic side chain, then undergoes further metabolism to polar carboxychromanols that are excreted in the urine. No other major human liver CYP enzymes exhibit this enzyme activity (*18*) and thus unlike many other CYP-catalyzed reactions, redundancy of function appears lacking. CYP4F2 exhibits pronounced substrate specificity among the various naturally occurring forms of vitamin E, such that those forms with incomplete methylation of the phenol ring or with unsaturated side chains are metabolized more rapidly (*15*). Consequently CYP4F2 appears to play a unique role in the post-absorptive catabolism of vitamin E that contributes, along with the hepatic α-TTP, to the widely-expressed phenotype of selective tissue deposition of α-tocopherol over other forms of vitamin E. Here we tested the hypothesis that two common mutations in the human *CYP4F2* gene would alter the activity of the enzyme toward vitamin E substrates. Consistent with this hypothesis, the W12G variant exhibited significantly greater ω-hydroxylase specific activity toward the three tocopherols tested and all the three tocotrienols tested. In sharp contrast, the V433M variant exhibited significantly lower specific activity toward the tocopherols, but was without significant effect with the tocotrienol substrates. Two tocopherols and one tocotrienol were also tested at lower concentrations, and the relative specific activities of the four enzyme isoforms were consistent across both substrate concentrations. All concentrations tested were either near or substantially below the apparent Km for tocopherol-ω-hydroxylase activity in human liver microsomes (*15*).

Our previous characterization of wild-type CYP4F2 activity toward a wide variety of naturally occurring and synthetic vitamin E substrates indicated that the tocotrienols were in general metabolized more readily than the tocopherols (*15*). The directionality of the effects of the two common SNP investigated here, in comparison to the wild-type enzyme, indicates that the tocotrienol-over-tocopherol substrate preference is retained, if not accentuated, in those variants. The biological rationale for the observed differences in catabolism of the different forms of vitamin E, even amongst the polymorphic forms of CYP4F2, remains an enigma. Accumulation of tocotrienols or tocopherols that are subject to higher rates of catabolism have been reported to result in beneficial effects in animal models (*32, 52, 53*) and cytotoxic effects in cell culture models (*54, 55*).

In the first reported investigation of the functional effects of the W12G and V433M variants of CYP4F2, Stec et al (*46*) reported a loss of arachidonic acid ω-hydroxylase activity by the V433M variant and a trend towards higher specific activity accompanying the W12G substitution. Both as a positive control for our findings with vitamin E and to re-evaluate the W12G variant in light of the substantial gain-of-function with both tocopherols and tocotrienols, we compared arachidonic acid ω-hydroxylase specific activity among the four enzyme isoforms. Under our experimental conditions, findings with the V433M variant and double mutant mirrored those reported previously, while the W12G variant exhibited a significant 2-fold enhancement of specific activity, similar to what was observed with the vitamin E substrates. The physiological significance of the latter finding is difficult to evaluate due to the redundancy in arachidonate 20-hydroxylase activity among multiple CYP450 enzymes, and the potential for compensatory degradation of 20-HETE.

The means by which these two amino acid substitutions act to affect enzyme function is unclear. The three dimensional structure of CYP4F2 has not been determined or modeled, thus the amino acid residues that participate in substrate binding, channeling and catalysis have not been identified. Sequence heterogeneity in the amino acid 67-114 region of CYP4F3A and CYP4F3B correlates with the differences in substrate specificity of these two 4F isoforms, suggesting this region may play a critical role in determining substrate specificity of other CYP4F enzymes (*24*), but neither of the current substitutions lie within this putative substrate recognition domain. Other possibilities include alterations in protein structure that affect how the enzyme orients in the membrane, which may in turn influence the access by membrane-bound substrates like vitamin E. Different forms of vitamin E may reside at different depths in biological membranes (*56*).

The impact of these two variations in CYP4F2 structure on vitamin E status in humans is at present unknown. Both of the naturally-occurring variants are relatively common in European-American and African-American derived sampling panels, as well as in the Chinese and Japanese HapMap dataset (*46*). In vivo investigations indicate that decreased CYP4F2 activity results in altered vitamin E status. Yamashita et al (*57*) reported that dietary sesamin, a sesame seed lignan later found to be an inhibitor of CYP4F2 (*35*), resulted in elevated concentrations of α- and γ-tocopherols in rat serum. Additionally, short-term administration of moderate amounts of sesame seeds to humans resulted in elevations in serum γ-tocopherol levels (*36*). These findings raise the distinct possibility that the CYP4F2 variants investigated here may contribute to variation in vitamin E status. Plasma α-tocopherol levels and responses to vitamin E supplementation are consistent over time within individuals, yet highly variable between individuals, leading to the suggestion that α-tocopherol status is influenced by genetic factors

(*44*). Individuals carrying one or two of the V433M variant alleles may exhibit increased plasma and tissue levels of tocopherols, and display a more pronounced response to tocopherol supplementation than individuals carrying wild-type alleles. In contrast, individuals carrying the W12G allele may display lower plasma and tissue levels of tocopherols, and little or no change in response to tocopherol or tocotrienol supplementation. Underlying genetic variability in vitamin E status and response to supplementation may contribute to inconsistent and null findings in both epidemiological and randomized controlled trials regarding vitamin E status and its relationship to disease risk. These possibilities are currently under investigation.

In conclusion, two common non-synonymous SNP in the *CYP4F2* gene cause significant alterations in vitamin E-ω-hydroxylase specific activity in a variant-dependent manner. The W12G variant exhibited increased enzyme activity toward both tocopherols and tocotrienols, while the V433M variant exhibited reduced enzyme activity towards tocopherols but not tocotrienols. The effect of these SNP on vitamin E status and response to vitamin E supplementation in humans has significant clinical implications and should be investigated.

CONCLUSION

Vitamin E is considered to be the most important lipid-soluble antioxidant in cell membranes and lipid stores. As such, the essentiality of vitamin E for fertility and central nervous system function has been well demonstrated. Despite the wealth of knowledge assembled over the decades, there are still aspects of vitamin E metabolism and function that are unknown. Because of the hepatic α-TTP which preferentially binds to α-TOH (*in vitro*), and the TOH-ω-oxidation pathway, which preferentially metabolizes non-α-TOH forms of vitamin E, there has never been a model in which to study the biological effects of non-α-TOH forms in vivo. In addition, the importance of the TOH-ω-oxidation pathway in maintaining the α-TOH phenotype has never been established in vivo, and the presence of other pathways of vitamin E metabolism have yet to be identified. Therefore, a mouse model was created, which would clarify the importance of the TOH-ω-oxidation pathway in vitamin E metabolism and status. This model would additionally allow the manipulation of vitamin E status such that the biological effects of forms that do not normally accumulate could be investigated.

CYP4F2 is the only known human enzyme shown to display TOH-ω-hydroxylase activity (*14*). Through this work, the functional murine ortholog of *CYP4F2* was identified and the consequences of its deletion on vitamin E metabolism and status were determined. As hypothesized, CYP4F14 was the major vitamin E-ω-hydroxylase, responsible for as much as 90% of the metabolic activity in the mouse. CYP4F14, however, was not the only enzyme capable of this activity as knockout mice were still excreting ω-hydroxy metabolites via both the urine and the feces. The enzyme(s) responsible for this redundant TOH-ω-hydroxylase activity are currently unknown. CYP4F14 was shown to have critical function in regulating body-wide vitamin E status, even under generally typical dietary conditions. Disruption of *Cyp4f14*

expression resulted in hyper-accumulation of γ-TOH in plasma and tissues in mice fed a diet similar in tocopherol composition to that consumed by many human populations.

Because of the experimental design of this study and the analytical capabilities used, several novel and important discoveries were made that were not initially envisioned. Firstly, the fecal route of metabolite excretion was found to be as important, if not more important, than the urinary route of vitamin E metabolite excretion. This work was the first to show not only the presence of vitamin E metabolites in feces, but also the quantitative importance of these metabolites. Secondly, two novel vitamin E metabolites were discovered, arising from ω-1 and ω-2 hydroxylation events. These novel pathways make up two of the three currently known enzyme-mediated pathways of vitamin E metabolism. Through metabolic cages studies, a substantial amount of unmetabolized TOHs were found in the feces of mice. Interestingly, both the fecal excretion of ω-1 and ω-2 metabolites as well as the fecal excretion of unmetabolized TOHs were higher in *Cyp4f14*$^{-/-}$ mice, somewhat counterbalancing the loss of vitamin E metabolic function. Redundancy in vitamin E-ω-hydroxylase activity and the existence of counterbalancing mechanisms implies a fundamental biological advantage of resisting diet-induced accumulation of non-α-TOH forms and maintenance of the α-TOH phenotype. As a result of this work, a new model of vitamin E metabolism has been established (**Fig. C.1**) with three possible metabolic fates of TOHs: ω-0 (13') hydroxylation, ω-1 (12') hydroxylation, or ω-2 (11') hydroxylation. While the 13'-OH metabolite can proceed through the ω-oxidation pathway, the 12'-OH metabolite is a terminal product. Whether the 11'-OH metabolite can be further oxidized is not currently known.

Cyp4f14$^{-/-}$ mice were physiologically normal despite the deficit in vitamin E metabolism, although longer term studies have yet to be conducted. A major question that still remained was

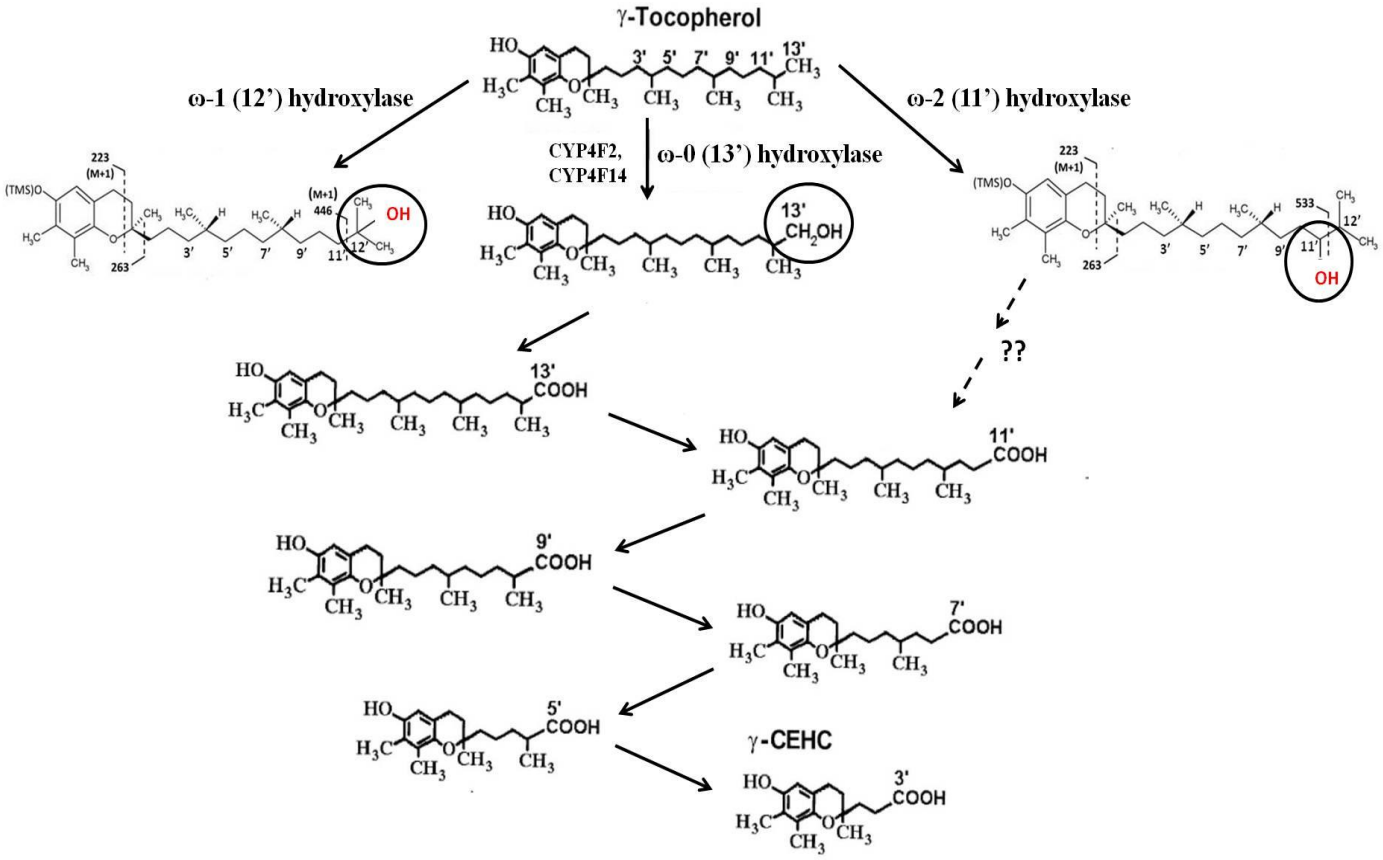

Figure C.1: Enzyme-mediated metabolism of vitamin E. Three pathways of enzyme-mediated catabolism are currently known. Tocopherols can be ω-hydroxylated by CYP4F2 (human) and CYP4F14 (mouse) and further oxidized through the ω-oxidation pathway. All intermediates can be excreted in the feces while only the two smallest-chain metabolites are found in the urine. Additionally, tocopherols can undergo ω-1 and ω-2 hydroxylation, the products of which are excreted via the feces.

what would occur if these mice were challenged with very high dietary levels of vitamin E forms that are normally cleared via the TOH-ω-oxidation pathway. To answer this question, *Cyp4f14*$^{-/-}$ mice were supplemented with γ- and δ-TOH in order to determine if a dietary challenge would allow for higher accumulation of these forms and to assess the physiolocal effect of this accumulation. Supplementation with γ- and δ-TOHs resulted in substantial increases in tissue levels of these forms in both wild-type and knockout mice relative to mice previously fed a soybean oil diet. While the fold-difference in tissue γ- and δ-TOHs between knockout and wild-

type mice was similar to that previously observed in unsupplemented mice, the absolute difference in tissue levels was substantially greater, as expected. Thus, the combination of supplementation and *Cyp4f14* disruption resulted in substantial tissue enrichment of TOHs, illustrating the potential of this model to study the biological consequences of tissue enrichment with specific forms of vitamin E. In supplemented *Cyp4f14*$^{-/-}$ mice, greater amounts of ω-1 and ω-2 metabolites were being excreted, indicating that the counterbalancing effect of these alternative pathways was still an important mechanism in limiting tissue TOH accumulation in the context of supplementation. In contrast to what is seen in the unsupplemented state, the excretion of unmetabolized TOHs did not constitute a counterbalancing effect in the *Cyp4f14*$^{-/-}$ mice, as the levels of these TOHs in the feces was not different between genotypes. However, in the supplemented state, fecal TOH elimination was a more important means of disposal of dietary TOHs than was metabolic elimination in both genotypes. In this respect, fecal elimination of unmetabolized TOHs serves as a high capacity mechanism of resisting tissue accumulation of dietary TOHs under conditions of supplementation. These findings suggest that supplementation was not able to completely overcome the mechanisms of resistance of tissue accumulation constituted by vitamin E metabolism and fecal TOH excretion

Presuming that all of the ω-0, ω-1, and ω-2 activities were present predominantly in the liver, a mouse model in which there was no CYP activity in the liver due to the liver-specific disruption of *Cpr* was utilized for further study. These mice were supplemented with δ- and γ-TOH, in an attempted to disable the mechanisms that were working against accumulation of non-α-TOHs. L-*Cpr*$^{-/-}$ mice fed the supplemented diet displayed substantial reduction in vitamin E metabolite excretion compared to wild-type mice. Unexpectedly, however, vitamin E metabolism was still present in these mice, revealing the presence of extra-hepatic vitamin E

metabolism, including ω-0, ω-1, and ω-2 activities. Due to an the major disruption of bile acid synthesis and subsequent inability to absorb lipids, L-*Cpr*-null mice had lower tissue levels of vitamin E compared to wild-type mice. Thus, the effect of complete disruption of hepatic vitamin E hydroxylase disruption on tissue TOH status could not be investigated. This model was, however, very useful in studying the site of extra-hepatic vitamin E metabolism. Microsomes from mouse small intestine mucosa of L-$Cpr^{-/-}$ mice displayed TOH-ω-hydroxylase activity toward α-, δ-, and γ-TOHs. The capability of vitamin E metabolism in these non-hepatic tissues is an extremely novel and important finding which deserves future attention.

While observations in mice do not always reflect similar processes in humans, many of the findings made through the use of these two knockout mouse models were validated in humans. Analysis of pooled human small intestinal mucosa microsomes demonstrated intestinal TOH-ω-hydroxylase activity to be present in the human as well as the mouse. In mice, the fecal route of metabolite excretion was found to be a major route of vitamin E metabolite excretion, a fact not previously known. In humans, fecal metabolites of α- and γ-TOH were also observed and should be taken into consideration in future studies of vitamin E metabolism. Novel metabolites of α- and γ-TOH from the ω-1 and ω-2 pathways were observed in human fecal material, revealing two novel pathways of vitamin E metabolism in humans. These pathways are quantitatively important pathways of vitamin E metabolism and warrant future research to elucidate the enzyme(s) responsible and the location of these pathways. Factors affecting the expression or activity of these enzyme(s) should also be studied, as alterations in vitamin E metabolism may lead to differences in vitamin E status as well as the effect of vitamin E intake on disease risk and prevention.

Through this work, the TOH-ω-oxidation pathway was found to play an important role in vitamin E status under typical dietary conditions. Therefore, two common mutations in the human *CYP4F2* gene were studied in a cell culture model in which the wild-type and polymorphic genes were separately expressed. The functional impact of these SNPs on TOH-ω-hydroxylase activity was studied. The W12G variant exhibited significantly greater ω-hydroxylase specific activity toward the three tocopherols tested and all the three tocotrienols tested. In sharp contrast, the V433M variant exhibited significantly lower specific activity toward the tocopherols, but was without significant effect with the tocotrienol substrates. These findings raise the distinct possibility that the CYP4F2 variants investigated here may contribute to variation in vitamin E status. Individuals carrying one or two of the V433M variant alleles may exhibit increased plasma and tissue levels of tocopherols, and display a more pronounced response to tocopherol supplementation than individuals carrying wild-type alleles. In contrast, individuals carrying the W12G allele may display lower plasma and tissue levels of tocopherols, and little or no change in response to tocopherol or tocotrienol supplementation. Underlying genetic variability in vitamin E status and response to supplementation may contribute to inconsistent and null findings in both epidemiological and randomized controlled trials regarding vitamin E status and its relationship to disease risk. In line with these findings, the V433M genotype was recently associated with higher circulating α-TOH concentrations (*37*) as well as response to α-TOH supplementation (*58*), further supporting the importance of *CYP4F2* and TOH-ω-hydroxylase activity in vitamin E status.

This work provides several interesting areas for future study. The atypical tissue accumulation of non-α-TOH forms of vitamin E in tocopherol supplemented *Cyp4f14*-null mice established this model as a useful model for studying the biological actions of these compounds.

Long-term studies should be conducted to determine the physiological effects of non-α-TOH tissue accumulation over a lifetime, including reproductive potential. Additionally, supplemented *Cyp4f14*-null mice can be exposed to various stresses and/or disease states to further assess the biological actions of vitamin E, beneficial or detrimental. Supplemental levels of tocotrienols should also be fed to *Cyp4f14*-null mice, and the metabolism and tissue accumulation of these forms should be studied in this context. These forms may be the most likely to have detrimental physiological effects, as they do not typically accumulate to any significant extent. Additionally, as CYP4F2 has been reported to have vitamin K metabolic activity, *Cyp4f14*$^{-/-}$ mice should be utilized to further explore the role of CYP4F14 in vitamin K metabolism and status. Other future studies involve the determination of the enzyme(s) responsible for the non-CYP4F14 dependent vitamin E-hydroxylase activities, including ω-0, ω-1, and ω-2 activities. These enzymes have been shown here to play an important role in vitamin E status, and deserve future attention. A comprehensive evaluation of extra-hepatic tissues for vitamin E metabolic activities should be conducted, including the adipose tissue which displays a different pattern of tocopherol composition compared to other tissues. Lastly, mice with intestinal-specific *Cpr* disruption should be utilized to determine the relative importance of intestinal vitamin E-hydroxylase activity to whole-body vitamin E metabolism.

Overall, the current works lends new insights into the TOH-ω-oxidation pathway as well as reveals novel pathways of vitamin E metabolism that are present in both mice and humans and play an important role in the regulation of vitamin E status. This work advances the field of vitamin E metabolism and provides new directions of future study.

REFERENCES

1. Barrie, M. M. (1938) Vitamin E deficiency in the rat: Fertility in the female, *Biochem J 32*, 2134-2137.

2. Yoshida, Y., Niki, E., and Noguchi, N. (2003) Comparative study on the action of tocopherols and tocotrienols as antioxidant: chemical and physical effects, *Chem Phys Lipids 123*, 63-75.

3. Saito, Y., Yoshida, Y., Akazawa, T., Takahashi, K., and Niki, E. (2003) Cell death caused by selenium deficiency and protective effect of antioxidants, *J Biol Chem 278*, 39428-39434.

4. Dial S, E. R. (1995) Tocopherols and tocotrienols in key foods in the US diet, In *Nutrition, Lipids, Health, and Disease* (Ong ASH, N. E., Packer L, Ed.), pp 327–342, AOCS Press, Champaign.

5. Bieri, J. G., and Evarts, R. P. (1973) Tocopherols and fatty acids in American diets. The recommended allowance for vitamin E, *J Am Diet Assoc 62*, 147-151.

6. Ford, E. S., Schleicher, R. L., Mokdad, A. H., Ajani, U. A., and Liu, S. M. (2006) Distribution of serum concentrations of alpha-tocopherol and gamma-tocopherol in the US population, *American Journal of Clinical Nutrition 84*, 375-383.

7. Manor, D., and Morley, S. (2007) The alpha-tocopherol transfer protein, *Vitam Horm 76*, 45-65.

8. Morley, S., Cecchini, M., Zhang, W., Virgulti, A., Noy, N., Atkinson, J., and Manor, D. (2008) Mechanisms of ligand transfer by the hepatic tocopherol transfer protein, *J Biol Chem 283*, 17797-17804.

9. Hosomi, A., Arita, M., Sato, Y., Kiyose, C., Ueda, T., Igarashi, O., Arai, H., and Inoue, K. (1997) Affinity for alpha-tocopherol transfer protein as a determinant of the biological activities of vitamin E analogs, *FEBS Lett 409*, 105-108.

10. Terasawa, Y., Ladha, Z., Leonard, S. W., Morrow, J. D., Newland, D., Sanan, D., Packer, L., Traber, M. G., and Farese, R. V., Jr. (2000) Increased atherosclerosis in

hyperlipidemic mice deficient in alpha -tocopherol transfer protein and vitamin E, *Proc Natl Acad Sci U S A 97*, 13830-13834.

11. Leonard, S. W., Terasawa, Y., Farese, R. V., Jr., and Traber, M. G. (2002) Incorporation of deuterated RRR- or all-rac-alpha-tocopherol in plasma and tissues of alpha-tocopherol transfer protein--null mice, *Am J Clin Nutr 75*, 555-560.

12. Lim, Y., and Traber, M. G. (2007) Alpha-Tocopherol Transfer Protein (alpha-TTP): Insights from Alpha-Tocopherol Transfer Protein Knockout Mice, *Nutr Res Pract 1*, 247-253.

13. Ouahchi, K., Arita, M., Kayden, H., Hentati, F., Ben Hamida, M., Sokol, R., Arai, H., Inoue, K., Mandel, J. L., and Koenig, M. (1995) Ataxia with isolated vitamin E deficiency is caused by mutations in the alpha-tocopherol transfer protein, *Nat Genet 9*, 141-145.

14. Parker, R. S., Sontag, T. J., Swanson, J. E., and McCormick, C. C. (2004) Discovery, characterization, and significance of the cytochrome P450 omega-hydroxylase pathway of vitamin E catabolism, *Ann N Y Acad Sci 1031*, 13-21.

15. Sontag, T. J., and Parker, R. S. (2007) Influence of major structural features of tocopherols and tocotrienols on their omega-oxidation by tocopherol-omega-hydroxylase, *J Lipid Res 48*, 1090-1098.

16. Traber, M. G., Sokol, R. J., Burton, G. W., Ingold, K. U., Papas, A. M., Huffaker, J. E., and Kayden, H. J. (1990) Impaired ability of patients with familial isolated vitamin E deficiency to incorporate alpha-tocopherol into lipoproteins secreted by the liver, *J Clin Invest 85*, 397-407.

17. Parker, R. S., and McCormick, C. C. (2005) Selective accumulation of alpha-tocopherol in Drosophila is associated with cytochrome P450 tocopherol-omega-hydroxylase activity but not alpha-tocopherol transfer protein, *Biochem Biophys Res Commun 338*, 1537-1541.

18. Sontag, T. J., and Parker, R. S. (2002) Cytochrome P450 omega-hydroxylase pathway of tocopherol catabolism. Novel mechanism of regulation of vitamin E status, *J Biol Chem 277*, 25290-25296.

19. Schonfeld, A., Schultz, M., Petrizka, M., and Gassmann, B. (1993) A novel metabolite of RRR-alpha-tocopherol in human urine, *Nahrung 37*, 498-500.

20. Wechter, W. J., Kantoci, D., Murray, E. D., Jr., D'Amico, D. C., Jung, M. E., and Wang, W. H. (1996) A new endogenous natriuretic factor: LLU-alpha, *Proc Natl Acad Sci U S A 93*, 6002-6007.

21. Swanson, J. E., Ben, R. N., Burton, G. W., and Parker, R. S. (1999) Urinary excretion of 2,7, 8-trimethyl-2-(beta-carboxyethyl)-6-hydroxychroman is a major route of elimination of gamma-tocopherol in humans, *J Lipid Res 40*, 665-671.

22. Nishimura, M., Yaguti, H., Yoshitsugu, H., Naito, S., and Satoh, T. (2003) Tissue distribution of mRNA expression of human cytochrome P450 isoforms assessed by high-sensitivity real-time reverse transcription PCR, *Yakugaku Zasshi 123*, 369-375.

23. Kikuta, Y., Kusunose, E., and Kusunose, M. (2002) Prostaglandin and leukotriene omega-hydroxylases, *Prostaglandins Other Lipid Mediat 68-69*, 345-362.

24. Christmas, P., Jones, J. P., Patten, C. J., Rock, D. A., Zheng, Y., Cheng, S. M., Weber, B. M., Carlesso, N., Scadden, D. T., Rettie, A. E., and Soberman, R. J. (2001) Alternative splicing determines the function of CYP4F3 by switching substrate specificity, *J Biol Chem 276*, 38166-38172.

25. Christmas, P., Tolentino, K., Primo, V., Berry, K. Z., Murphy, R. C., Chen, M., Lee, D. M., and Soberman, R. J. (2006) Cytochrome P-450 4F18 is the leukotriene B4 omega-1/omega-2 hydroxylase in mouse polymorphonuclear leukocytes: identification as the functional orthologue of human polymorphonuclear leukocyte CYP4F3A in the down-regulation of responses to LTB4, *J Biol Chem 281*, 7189-7196.

26. Kikuta, Y., Kasyu, H., Kusunose, E., and Kusunose, M. (2000) Expression and catalytic activity of mouse leukotriene B4 omega-hydroxylase, CYP4F14, *Arch Biochem Biophys 383*, 225-232.

27. Parker, R. S., and Swanson, J. E. (2000) A novel 5'-carboxychroman metabolite of gamma-tocopherol secreted by HepG2 cells and excreted in human urine, *Biochem Biophys Res Commun 269*, 580-583.

28. Truett, G. E., Heeger, P., Mynatt, R. L., Truett, A. A., Walker, J. A., and Warman, M. L. (2000) Preparation of PCR-quality mouse genomic DNA with hot sodium hydroxide and tris (HotSHOT), *Biotechniques 29*, 52, 54.

29. You, C. S., Sontag, T. J., Swanson, J. E., and Parker, R. S. (2005) Long-chain carboxychromanols are the major metabolites of tocopherols and tocotrienols in A549 lung epithelial cells but not HepG2 cells, *J Nutr 135*, 227-232.

30. Yamane, M., and Abe, A. (2000) omega-hydroxylation activity toward leukotriene B(4) and polyunsaturated fatty acids in the human hepatoblastoma cell line, HepG2, and human lung adenocarcinoma cell line, A549, *J Biochem 128*, 827-835.

31. Traber, M. G., and Arai, H. (1999) Molecular mechanisms of vitamin E transport, *Annu Rev Nutr 19*, 343-355.

32. Jiang, Q., Lykkesfeldt, J., Shigenaga, M. K., Shigeno, E. T., Christen, S., and Ames, B. N. (2002) Gamma-tocopherol supplementation inhibits protein nitration and ascorbate oxidation in rats with inflammation, *Free Radic Biol Med 33*, 1534-1542.

33. Zhao, Y., Lee, M. J., Cheung, C., Ju, J. H., Chen, Y. K., Liu, B., Hu, L. Q., and Yang, C. S. (2010) Analysis of multiple metabolites of tocopherols and tocotrienols in mice and humans, *J Agric Food Chem 58*, 4844-4852.

34. Mustacich, D. J., Gohil, K., Bruno, R. S., Yan, M., Leonard, S. W., Ho, E., Cross, C. E., and Traber, M. G. (2009) Alpha-tocopherol modulates genes involved in hepatic xenobiotic pathways in mice, *J Nutr Biochem 20*, 469-476.

35. Parker, R. S., Sontag, T. J., and Swanson, J. E. (2000) Cytochrome P4503A-dependent metabolism of tocopherols and inhibition by sesamin, *Biochem Biophys Res Commun 277*, 531-534.

36. Cooney, R. V., Custer, L. J., Okinaka, L., and Franke, A. A. (2001) Effects of dietary sesame seeds on plasma tocopherol levels, *Nutr Cancer 39*, 66-71.

37. Major, J. M., Yu, K., Wheeler, W., Zhang, H., Cornelis, M. C., Wright, M. E., Yeager, M., Snyder, K., Weinstein, S. J., Mondul, A., Eliassen, H., Purdue, M., Hazra, A., McCarty, C. A., Hendrickson, S., Virtamo, J., Hunter, D., Chanock, S., Kraft, P., and Albanes, D. (2011) Genome-wide association study identifies common variants associated with circulating vitamin E levels, *Hum Mol Genet 20*, 3876-3883.

38. Bardowell, S. A., Stec, D. E., and Parker, R. S. (2010) Common variants of cytochrome P450 4F2 exhibit altered vitamin E-{omega}-hydroxylase specific activity, *J Nutr 140*, 1901-1906.

39. Bardowell, S. A., Duan, F., Manor, D., Swanson, J. E., and Parker, R. S. (2012) Disruption of mouse cytochrome P450 4f14 (Cyp4f14) causes severe perturbations in vitamin E metabolism, *J Biol Chem*.

40. Gu, J., Weng, Y., Zhang, Q. Y., Cui, H., Behr, M., Wu, L., Yang, W., Zhang, L., and Ding, X. (2003) Liver-specific deletion of the NADPH-cytochrome P450 reductase gene: impact on plasma cholesterol homeostasis and the function and regulation of microsomal cytochrome P450 and heme oxygenase, *J Biol Chem 278*, 25895-25901.

41. Henderson, C. J., Otto, D. M., Carrie, D., Magnuson, M. A., McLaren, A. W., Rosewell, I., and Wolf, C. R. (2003) Inactivation of the hepatic cytochrome P450 system by conditional deletion of hepatic cytochrome P450 reductase, *J Biol Chem 278*, 13480-13486.

42. Kikuta, Y., Kusunose, E., Kondo, T., Yamamoto, S., Kinoshita, H., and Kusunose, M. (1994) Cloning and expression of a novel form of leukotriene B4 omega-hydroxylase from human liver, *FEBS Lett 348*, 70-74.

43. Powell, P. K., Wolf, I., Jin, R., and Lasker, J. M. (1998) Metabolism of arachidonic acid to 20-hydroxy-5,8,11, 14-eicosatetraenoic acid by P450 enzymes in human liver: involvement of CYP4F2 and CYP4A11, *J Pharmacol Exp Ther 285*, 1327-1336.

44. Kelly, F. J., Lee, R., and Mudway, I. S. (2004) Inter- and intra-individual vitamin E uptake in healthy subjects is highly repeatable across a wide supplementation dose range, *Ann N Y Acad Sci 1031*, 22-39.

45. Doring, F., Rimbach, G., and Lodge, J. K. (2004) In silico search for single nucleotide polymorphisms in genes important in vitamin E homeostasis, *Iubmb Life 56*, 615-620.

46. Stec, D. E., Roman, R. J., Flasch, A., and Rieder, M. J. (2007) Functional polymorphism in human CYP4F2 decreases 20-HETE production, *Physiol Genomics 30*, 74-81.

47. Caldwell, M. D., Awad, T., Johnson, J. A., Gage, B. F., Falkowski, M., Gardina, P., Hubbard, J., Turpaz, Y., Langaee, T. Y., Eby, C., King, C. R., Brower, A., Schmelzer, J.

R., Glurich, I., Vidaillet, H. J., Yale, S. H., Qi Zhang, K., Berg, R. L., and Burmester, J. K. (2008) CYP4F2 genetic variant alters required warfarin dose, *Blood 111*, 4106-4112.

48. Fava, C., Montagnana, M., Almgren, P., Rosberg, L., Lippi, G., Hedblad, B., Engstrom, G., Berglund, G., Minuz, P., and Melander, O. (2008) The V433M variant of the CYP4F2 is associated with ischemic stroke in male Swedes beyond its effect on blood pressure, *Hypertension 52*, 373-380.

49. Deng, S., Zhu, G., Liu, F., Zhang, H., Qin, X., Li, L., and Zhiyi, H. CYP4F2 gene V433M polymorphism is associated with ischemic stroke in the male Northern Chinese Han population, *Prog Neuropsychopharmacol Biol Psychiatry 34*, 664-668.

50. Ding, H., Cui, G., Zhang, L., Xu, Y., Bao, X., Tu, Y., Wu, B., Wang, Q., Hui, R., Wang, W., Dackor, R. T., Kissling, G. E., Zeldin, D. C., and Wang, D. W. Association of common variants of CYP4A11 and CYP4F2 with stroke in the Han Chinese population, *Pharmacogenet Genomics 20*, 187-194.

51. McDonald, M. G., Rieder, M. J., Nakano, M., Hsia, C. K., and Rettie, A. E. (2009) CYP4F2 is a vitamin K1 oxidase: An explanation for altered warfarin dose in carriers of the V433M variant, *Mol Pharmacol 75*, 1337-1346.

52. Jiang, Q., and Ames, B. N. (2003) gamma-Tocopherol, but not alpha-tocopherol, decreases proinflammatory eicosanoids and inflammation damage in rats, *Faseb Journal 17*, 816-822.

53. Khanna, S., Roy, S., Slivka, A., Craft, T. K., Chaki, S., Rink, C., Notestine, M. A., DeVries, A. C., Parinandi, N. L., and Sen, C. K. (2005) Neuroprotective properties of the natural vitamin E alpha-tocotrienol, *Stroke 36*, 2258-2264.

54. McCormick, C. C., and Parker, R. S. (2004) The cytotoxicity of vitamin E is both vitamer- and cell-specific and involves a selectable trait, *J Nutr 134*, 3335-3342.

55. You, C. S., McCormick, C. C., and Parker, R. S. (2004) Metabolism and cytotoxicity of tocopherols and tocotrienols in human type II (A549) pneumocytes, *Faseb Journal 18*, A159-A159.

56. Grau, A., and Ortiz, A. (1998) Dissimilar protection of tocopherol isomers against membrane hydrolysis by phospholipase A2, *Chem Phys Lipids 91*, 109-118.

57. Yamashita, K., Iizuka, Y., Imai, T., and Namiki, M. (1995) Sesame seed and its lignans produce marked enhancement of vitamin E activity in rats fed a low alpha-tocopherol diet, *Lipids 30*, 1019-1028.

58. Major, J. M., Yu, K., Chung, C. C., Weinstein, S. J., Yeager, M., Wheeler, W., Snyder, K., Wright, M. E., Virtamo, J., Chanock, S., and Albanes, D. (2012) Genome-wide association study identifies three common variants associated with serologic response to vitamin E supplementation in men, *J Nutr 142*, 866-871.